Manuscript Details

Manuscript number	DSR2_2017_210_R2
Title	Diatom species fluxes in the seasonally ice-covered Antarctic Zone: new data from offshore Prydz Bay and comparison with other regions from the eastern Antarctic and western Pacific sectors of the Southern Ocean.
Article type	Full length article

Abstract

The Antarctic Zone, the southernmost belt of the Antarctic Circumpolar Current, plays an important role in the control of atmospheric carbon dioxide concentrations. In the last decade, a number of studies have highlighted the importance of diatom assemblage composition in influencing the magnitude of the organic carbon and biogenic silica fluxes exported out of the mixed layer in Southern Ocean ecosystems. Here we investigate the relationship between the makeup of the diatom assemblage, organic carbon and biogenic silica export and several significant environmental parameters using sediment trap records deployed in different sectors of the Antarctic Zone. The study is divided in two parts. We first present unpublished diatom species flux data collected by a sediment trap in the offshore waters of Prydz Bay (Station PZB-1) over a year. The results of this study revealed a major export peak of diatom valves in Austral summer and two small unexpected secondary flux pulses during full winter conditions. The summer diatom sinking assemblages were largely composed of small and rapidly dividing species such as Fragilariopsis cylindrus, Fragilariopsis curta and Pseudo-nitzschia lineola, while winter assemblages were dominated by Fragilariopsis kerguelensis most reflecting its persistent strategy and selective preservation. In the second part of the study, we compare the annual diatom assemblage composition and biogeochemical fluxes of Station PZB-1 with flux data documented in previous sediment trap studies conducted in other sectors of the Antarctic Zone in order to investigate how diatom floristics influence the composition and magnitude of particle fluxes in the Antarctic Zone. The lack of correlation between the annual diatom valve, organic carbon and biogenic silica fluxes across stations indicates that other factors aside from diatom abundance play a major role in the carbon and silica export in AZ. Among these factors, the composition of the diatom assemblage appears to be critical, as suggested by the strong and significant correlation between Bio-SiO2 and the valve fluxes of F. kerguelensis alone, that this species is the main Bio-SiO2 vector from the surface layer to the deep ocean in the AZ waters, regardless of its relative abundance. Lastly, the good correlation between the annual fluxes of the group of small Fragilariopsis species with satellite-derived chlorophyll-a concentration estimates over the study stations, suggest that high abundances of these species in the Southern Ocean paleorecords could be used as a proxy of high algal biomass accumulation.

Corresponding Author	Andrés Rigual Hernández
Corresponding Author's Institution	Universidad de Salamanca
Order of Authors	Andrés Rigual Hernández, Cynthia Pilskaln, Aleix Cortina, Fatima Abrantes, Leanne L.K. Armand

Diatom species fluxes in the seasonally ice-covered Antarctic Zone: new data from offshore Prydz Bay and comparison with other regions from the eastern Antarctic and western Pacific sectors of the Southern Ocean.

Rigual-Hernández, A.S.[1], Pilskaln, C.H.[2], Cortina, A.[3], Abrantes, F.[4] and Armand, L.K.[5]

1 Área de Paleontología, Departamento de Geología, Universidad de Salamanca, 37008 Salamanca, Spain

2 School for Marine Science and Technology (SMAST), University of Massachusetts Dartmouth, New Bedford, MA, 02744, USA

3 Department of Environmental Chemistry, IDAEA-CSIC, 08034 Barcelona, Spain.

4 Portuguese Institute for Sea and Atmosphere (IPMA), Divisão de Geologia Marinha (DivGM), Rua Alferedo Magalhães Ramalho 6, Lisboa, Portugal

5 Research School of Earth Sciences, The Australian National University, 142 Mills Road Acton ACT 2601, Australia

*corresponding author. arigual@usal.es

Abstract

The Antarctic Zone, the southernmost belt of the Antarctic Circumpolar Current, plays an important role in the control of atmospheric carbon dioxide concentrations. In the last decade, a number of studies have highlighted the importance of diatom assemblage composition in influencing the magnitude of the organic carbon and biogenic silica fluxes exported out of the mixed layer in Southern Ocean ecosystems. Here we investigate the relationship between the makeup of the diatom assemblage, organic carbon and biogenic silica export and several significant environmental parameters using sediment trap records deployed in different sectors of the Antarctic Zone. The study is divided in two parts. We first present unpublished diatom species flux data collected by a sediment trap in the offshore waters of Prydz Bay (Station PZB-1) over a year. The results of this study revealed a major export peak of diatom valves in Austral summer and two small unexpected secondary flux pulses during full winter conditions. The summer diatom sinking assemblages were largely composed of small and rapidly dividing species such as *Fragilariopsis cylindrus*, *Fragilariopsis curta* and *Pseudo-nitzschia lineola*, while

winter assemblages were dominated by *Fragilariopsis kerguelensis* most reflecting its persistent strategy and selective preservation.

In the second part of the study, we compare the annual diatom assemblage composition and biogeochemical fluxes of Station PZB-1 with flux data documented in previous sediment trap studies conducted in other sectors of the Antarctic Zone in order to investigate how diatom floristics influence the composition and magnitude of particle fluxes in the Antarctic Zone. The lack of correlation between the annual diatom valve, organic carbon and biogenic silica fluxes across stations indicates that other factors aside from diatom abundance play a major role in the carbon and silica export in AZ. Among these factors, the composition of the diatom assemblage appears to be critical, as suggested by the strong and significant correlation between Bio-SiO_2 and the valve fluxes of *F. kerguelensis* alone, that this species is the main Bio-SiO_2 vector from the surface layer to the deep ocean in the AZ waters, regardless of its relative abundance. Lastly, the good correlation between the annual fluxes of the group of small *Fragilariopsis* species with satellite-derived chlorophyll-*a* concentration estimates over the study stations, suggest that high abundances of these species in the Southern Ocean paleorecords could be used as a proxy of high algal biomass accumulation.

1. Introduction

1. Southern Ocean phytoplankton

The Southern Ocean is a crucial component of the global overturning circulation and regulates the climate system through the uptake of heat, freshwater and atmospheric CO_2 (Sarmiento et al., 2004). Despite its relatively small size, it accounts for about 20% (0.47 $GtCyr^{-1}$) of the ocean CO_2 uptake flux (Takahashi et al., 2002). A significant fraction of the CO_2 drawdown in the Southern Ocean waters is driven by phytoplankton (Siegel et al., 2014)

Phytoplankton productivity is not sustained at its full capacity in the Southern Ocean in spite of the fact that concentrations of most macronutrients remain ubiquitously high, making the Southern Ocean the largest high-nutrient low-chlorophyll (HNLC) area of the global ocean. Numerous studies have conclusively demonstrated that Fe-limitation plays a critical role in restricting phytoplankton biomass and production within HNLC regions

of the Southern Ocean (Boyd and Law, 2001; Boyd et al., 2004; Coale et al., 2004 , among others). Indeed, it is likely that iron availability had played an important role in the variations of the atmospheric carbon dioxide levels over glacial cycles (Martínez-Garcia et al., 2009). Diatoms are the major primary producers in the Southern Ocean and are often reported dominating high-productivity events in the Polar Frontal Zone, Antarctic Zone (AZ) and coastal systems of Antarctica (e.g. Wilson et al., 1986; Bathmann et al., 1997; Arrigo et al., 1999; Selph et al., 2001; Landry et al., 2002). Diatom blooms account for a large fraction of the particulate organic carbon (POC) flux and for almost all of the biogenic silica export out of the mixed layer. This export can be direct through the formation of rapidly sinking aggregates of entangled cells and chains with fast sinking rates (Boyd and Newton, 1999; Smetacek et al., 2012) or indirect via the production of faecal material by zooplankton grazing of diatoms (Rembauville et al., 2014; Manno et al., 2015; Belcher et al., 2016). The large accumulation of siliceous diatom remains in the deep sea sediments between the winter sea ice edge and the Antarctic Polar Front is responsible for the formation of a circumpolar Diatom Ooze Belt in the Southern Ocean deep sea sediments (Burckle and Cirilli, 1987) that represents one of the most important silica sinks in the world ocean (Tréguer, 2014).

As a more complete understanding of Southern Ocean ecosystems is developed, it is becoming increasingly evident that the species composition of the plankton communities plays a critical role in the regulation of ocean nutrient stoichiometry at regional and global levels (e.g. Arrigo et al., 1999; Salter et al., 2014). More specifically, recent studies provided conclusive evidence that the ecological traits and strategies of different polar diatom species contribute to the regulation of the efficiency of the biological pump and the degree of coupling of the carbon and silicon in the particles sinking to the interior layers of the Southern Ocean (e.g. Salter et al., 2012; Assmy et al., 2013; Rembauville et al., 2014; Rigual-Hernández et al., 2015b). Although ocean colour satellites provide a circumpolar view of biological activity and some insights into the fractional contribution of major phytoplankton functional groups (e.g. coccolithophores, *Phaeocystis*-like, diatoms) to algal biomass accumulation (Alvain et al., 2008), they are unable to resolve the species composition of phytoplankton communities and seasonal species succession. *In situ* and year-round observations are therefore needed to refine the interpretations based on satellite data, to relate surface chlorophyll to column-integrated production and export and to determine the specific role of phytoplankton species in the

Southern Ocean ecosystems. Sediment trap mooring deployments are one direct method of characterizing and quantifying the biogeochemical composition of particle fluxes and allows for the determination of composition and seasonality of diatom sinking assemblages. This technology is particularly useful in remote regions of the Southern Ocean, such as those of AZ, which are often seasonally covered by sea ice.

The main goal of this study is to investigate the relationship between the diatom species flux assemblage, the POC and opal fluxes, and several significant environmental parameters across key regions of the AZ of the Eastern Antarctic and Western Pacific sectors of the Southern Ocean. The study is divided into two parts: firstly, we present unpublished data on the diatom species fluxes intercepted by a sediment trap over a year in the offshore waters of Prydz Bay. An improved understanding of the seasonality and environmental preferences of diatom species captured by the trap will allow for better interpretation of the paleorecords of the study region. Secondly, we compare the diatom flux assemblage and biogeochemical fluxes of Station PZB-1 with already published sediment trap data from other regions of the AZ. This comparison provides insight into how diatom floristics influence the composition and magnitude of particle fluxes across different sectors of the AZ.

1.2 The Antarctic Zone

The Southern Ocean is divided into a series of zonal systems characterized by relatively uniform chemical and physical properties. These zonal systems are separated by fronts that carry most of the transport of the Antarctic Circumpolar Current (ACC) (Nowlin and Clifford, 1982). The AZ represents the southernmost zonal system of the Antarctic Circumpolar Current and is delimited to the north by the Polar Front (PF) and to the south by the Southern Boundary (SBDY; Fig. 1). South of Kerguelen, the AZ is at its largest extent, while in other sectors it is only a few degrees wide (Fig. 1b). The AZ is characterized by a well-mixed surface layer (down to 150 m in winter) of cold Winter Water (WW) which is overlain by warmer and less saline Antarctic Surface Water (AASW) in the summer (Orsi et al., 1995; Chaigneau et al., 2004). The Southern Boundary of Upper Circumpolar Deepwater (SBDY or the Antarctic Divergence) represents the southern limit of the AZ where the atmospheric wind regime reverses into strong westerlies that drive a northward Ekman transport of deep, relatively warm and

nutrient-rich waters that upwell south of the APF (Speer et al., 2000; Pollard et al., 2006). The AZ can be broadly subdivided into a permanent ice-free zone (Permanently Open Ocean Zone, or POOZ) and a Seasonal Ice Zone (SIZ). The SIZ is limited in the north by the northern winter limit of the pack-ice and in the south by the northern summer limit of the pack-ice. The retreating sea ice edge during the summer exhibits one of the highest rates of primary production in the Southern Ocean (Arrigo et al., 2008) and accounts for an annual primary production of 86.7 ± 12.6 Tg C yr^{-1}. Diatom production and export to the deep sea is thought to be largely responsible for the Si concentration gradient across the AZ (Dugdale and Wilkerson, 2001; Assmy et al., 2013), from ~60 µmol kg^{-1} in the southern AZ due to the upwelling of Circumpolar Deep Waters, to < 10 µmol kg^{-1} north the Antarctic Polar Front (Coale et al., 2004; Bostock et al., 2013).

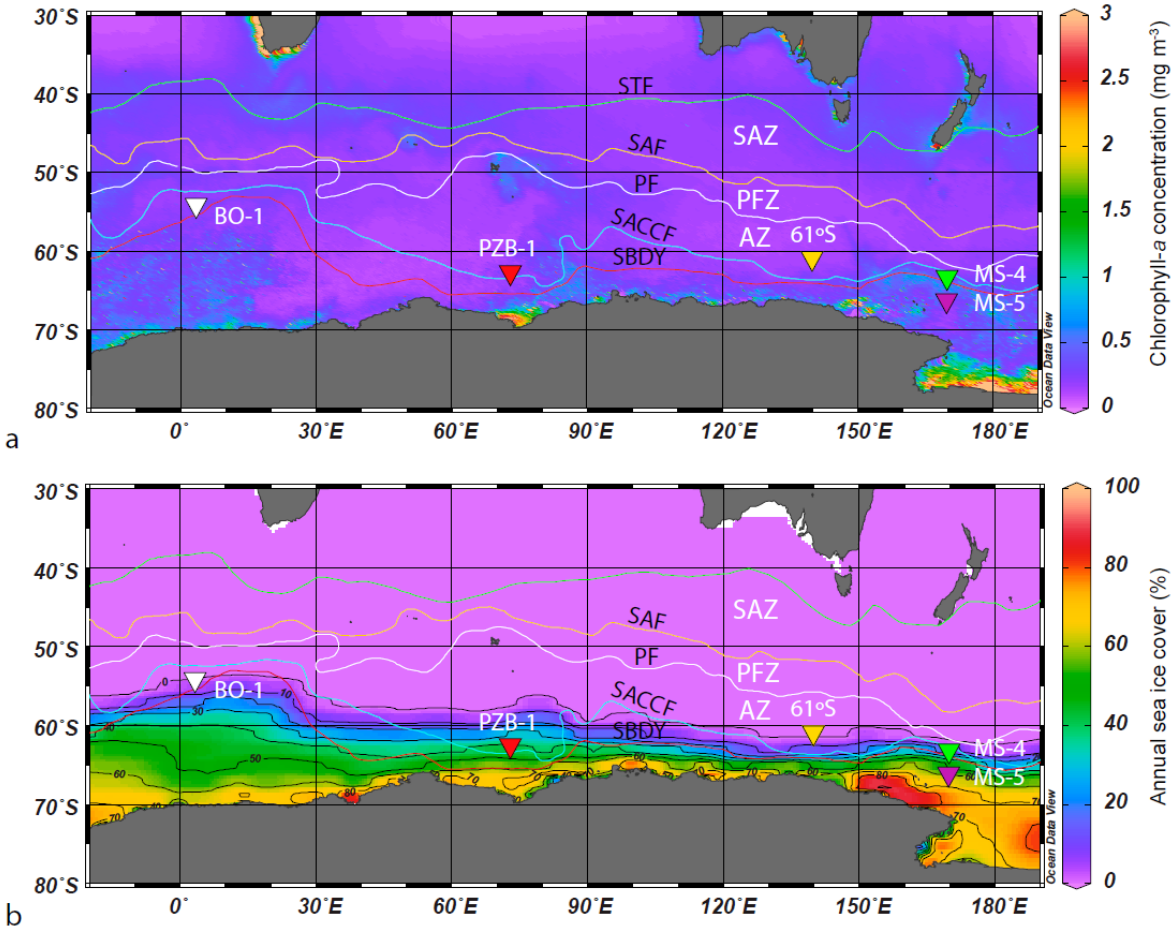

Figure 1. a Chlorophyll-*a* composite map (1997 to 2012) from Sea-viewing Wide Field-of-View Sensor (SeaWiFS) of the Southern Ocean. **b.** Area-Averaged of Percentage sea ice cover monthly between 1997 and 2012 from the Giovanni NASA portal. Location of the sediment trap moorings in the AZ discussed in this article: PZB-1, BO-1, 61°S, MS-4 and MS-5 stations (inverted triangles). Abbreviations: STF – Subtropical Front, SAZ –

Subantarctic Zone, SAF – Subantarctic Front, PFZ – Polar Frontal Zone, PF – Polar Front, AZ – Antarctic Zone, Southern ACC Front – SACCF, Southern Boundary of Upper Circumpolar Deepwater – SBDY. Oceanic fronts after Orsi et al. (1995).

2. Material and Methods

2.1 Field programs

2.1.1 Offshore Prydz Bay trap experiment

As part of a field research collaboration between the US and China polar research programs, a mooring equipped with three sediment traps (1400, 2400 and 3400 m depth) was deployed at 62°29'S; 72°59'E in the seasonal ice zone of the AZ north of Prydz Bay (station PZB-1) from December 1998 to December 1999 (Pilskaln et al., 2004; Fig. 1). All the sediment traps were McLane, Inc. time-series traps, with a 0.5 m^2 diameter opening and equipped with 13 cups (Honjo and Doherty, 1988). Due to a timer failure, no samples beyond cup 2 were collected by the 2400 m PZB-1 trap. Additionally, the material mass collected in the 3400 m PZB-1 trap cups was too small to allow for diatom counts after the priority geochemical analyses were completed (see Pilskaln et al. 2004 for details). Therefore, only data from the 1400 m is discussed here.

The sample cups were filled prior to the deployment with a 4% density-adjusted formalin solution in filtered seawater buffered to a pH of 7.8-8.1 (Honjo et al., 2000; Pilskaln et al., 2004). Cup rotation and collection intervals were established based on anticipated mass fluxes. The sampling intervals ranged from 17 days in austral spring and summer to a maximum collection interval of 41 days during the winter ice-cover month. A presentation and discussion of the geochemical fluxes and major planktonic contributions to settling particles at several trap depths in the offshore Prydz Bay region can be found in Pilskaln et al. (2004). Annual export fluxes at 1400 m were dominated by Bio-SiO_2 that represented 73% of the annual mass export. A detailed description of the diatom species analysis of the 1400 m time-series trap samples is provided in section 3.2.

2.1.2 Other sediment trap experiments in the AZ between 0-180°E

In the second part of the paper, biogeochemical and diatom species flux data from Station PZB-1 are compared with already published datasets from four sediment trap deployments (Table 1) in distinct settings of the AZ of the Southern Ocean (Fischer et al., 2002; Grigorov et al., 2014; Rigual-Hernández et al., 2015a). Next, we summarize the field experiments and the environmental conditions at each of the stations compared.

Station BO-1 (54° 20´S; 3° 23'E) was located in the eastern Atlantic Sector of the Southern Ocean, close to the northernmost winter sea-ice edge and about 4° north of the ACC-Weddell Gyre Boundary. The surface waters around station BO are characterized by high macronutrient concentrations (Fischer et al., 2002), low iron levels (Loscher et al., 1997) and low algal accumulation (Antoine et al., 1996; Arrigo et al., 2008). A mooring line equipped with two sediment traps, placed at ~500 and 2200 m below the surface (water column of 2700 m), was deployed over five almost consecutive years (1990-95). Fischer et al. (2002) reported biogeochemical data for the five deployments but diatom composition was only documented for year 1991. Bio-SiO_2 dominated the mass fluxes year-round, representing 64% of the annual total mass flux. Station BO-1 was under the influence of sea ice for about three months, from August to October 1991.

Station 61°S (60° 44.43´S; 139° 53.97´E) was located in the Australian sector of the southern AZ north of the Seasonal Ice Zone (Massom et al., 2013). Despite the high macronutrient concentrations (silicate, nitrate and phosphate), the waters in this region exhibit very low algal concentrations year-round (< 0.5 µg l-1; Popp et al., 1999; Parslow et al., 2001; Trull et al., 2001) most likely due to the very low iron concentrations (0.1-0.2 nM; Boyd et al., 2000). Station 61°S was equipped for a year (November 2001 to September 2002) with a mooring line with three sediment traps placed at 1000, 2000 and 3700 m below the surface in a water column of 4393 m. Due to equipment malfunction no samples were recovered from the 1000 m trap. Since the rest of the sediment traps compared here were deployed at shallower depths, only data from the shallowest trap (2000 m) are discussed here. Export fluxes were largely dominated by Bio-SiO_2 that accounted for 76% of the annual mass flux at 2000 m. A detailed description of the diatom valve and biogeochemical fluxes can be found in Rigual-Hernández et al. (2015a).

As part of the US-JGOFS Antarctic Environmental Southern Ocean Process Study (AESOPS; Smith Jr et al., 2000) and array of sediment traps was deployed along the 170°W parallel, in the western Pacific sector of the Southern Ocean (Honjo et al., 2000). Two sediment trap mooring lines with sediment traps placed at ~1000 and 2000 m depth

were deployed during a year at Stations MS-4 (63° 09´S; 169° 54´W) and MS-5 (66° 10´S; 169° 40´W), located south of the Antarctic Polar Front within the AZ. Because diatom species flux data were only available for the 1000 m traps, only data from these traps are discussed here. Station MS-4 was located south of the ACC while MS-5 was placed within the north of Ross Sea Gyre. The pelagic waters south of the Antarctic Polar Front in this region are characterized by high nutrient concentrations year-round and by the highest annual primary production values of the pelagic province of the Southern Ocean (Arrigo et al., 2008). Station MS-4 was under the influence of sea ice during about three months in winter, while the MS-5 mooring line was covered by ice during most of the year, except during three months in summer (Honjo et al., 2000). The episodic release of iron from the melting sea ice has been suggested as an important mechanism stimulating algal growth (predominantly diatoms) in the waters around Stations MS-4 and MS-5 (Sedwick and DiTullio, 1997; Grigorov et al., 2014). Detailed information on the biogeochemical and diatom flux data measured at the Stations MS-4 and MS-5 can be found in Honjo et al. (2000) and Grigorov et al. (2014), respectively. Annual export fluxes were dominated by Bio-SiO_2 at both Stations, accounting for 69% and 58% of the annual total mass flux at MS-4 and MS-5, respectively.

Station	Latitude	Longitude	Water column depth (m)	Trap depth (m)	Sampling interval start	Sampling interval end
BO-1	54° 20´S	3° 23'E	2734	450	28/12/1990	01/04/1992
PZB-1	62°29'S	72°59'E	4000	1400	30/12/1998	13/12/1999
61°S	60° 44´S	139° 54´E	4393	2000	30/11/2001	29/09/2002
MS-4	63° 09´S	169° 54´W	2885	1031	28/11/1996	24/12/1997
MS-5	66° 10´S	169° 40´W	3015	937	28/11/1996	24/12/1997

Table 1. Summary of mooring deployment locations, sediment trap depths and anchor depths.

2.2 Sample processing for diatom analysis

A detailed explanation of the sample preparation for diatom analysis for the PFZ-1 is provided next, together with brief summary of the sample processing used in the other sediment trap experiments. One quantitative wet-split fraction from each of the 1400 m trap cups was designated for diatom analysis. The sample aliquot was gently rinsed and filtered with distilled water to remove salt and formalin and then treated with potassium

permanganate and hydrochloric acid for the removal of organic and calcareous material according to the procedures detailed in Schrader and Gersonde (1978) and Romero (1998). A 150-300 µl drop of the remaining suspended siliceous material was placed on a coverslip in a settling chamber, using the random settling technique described in Moore (1973). Once dry, the coverslips were mounted on glass slides using a high refractive index mountant (Naphrax) for light microscopy counts and identification of diatoms. The total flux of diatoms to each cup in valves m^{-2} day^{-1} was calculated by multiplying the valve count by the area counted as a fraction of the total area and the dilution volume, all multiplied by the split and then divided by the collection period in days and the trap collection surface area (Sancetta and Calvert, 1988). The diatom species fluxes of the most abundant diatom species at PZB-1 are listed in Table 2 and plotted in Figure 2.

Table 2: Diatom species fluxes of the most abundant diatom species for the deployment PZB-1 (1400 m trap).

Cup number	Mid-point date	Collection days (days)	Total diatom flux (10^6 x valves m^{-2} d^{-1})	*Fragilariopsis curta* (10^6 x valves m^{-2} d^{-1})	*Fragilariopsis cylindrus* (10^6 x valves m^{-2} d^{-1})	*Fragilariopsis kerguelensis* (10^6 x valves m^{-2} d^{-1})	*Fragilariopsis pseudonana* (10^6 x valves m^{-2} d^{-1})	*Fragilariopsis rhombica* (10^6 x valves m^{-2} d^{-1})	*Pseudo-nitzschia lineola* (10^6 x valves m^{-2} d^{-1})	*Thalassisora gracilis* var. *expecta* (10^6 x valves m^{-2} d^{-1})	*Thalassiosira lentiginosa* (10^6 x valves m^{-2} d^{-1})
1	07/01/1999	17.0	128.6	15.8	35.5	16.6	3.7	8.3	14.6	4.9	0.9
2	25/01/1999	19.0	284.6	28.2	101.6	30.1	16.9	23.8	41.1	12.5	0.6
3	12/02/1999	17.0	37.2	2.6	9.0	9.0	0.7	3.6	2.5	2.5	0.2
4	01/03/1999	17.0	23.4	2.2	2.2	9.3	0.3	1.8	1.5	2.5	0.5
5	18/03/1999	17.0	1.5	0.1	0.0	0.9	0.0	0.1	0.0	0.1	0.1
6	16/04/1999	40.0	1.5	0.1	0.0	0.8	0.0	0.1	0.0	0.2	0.0
7	26/05/1999	41.0	1.4	0.1	0.0	0.6	0.0	0.1	0.0	0.2	0.0
8	06/07/1999	41.0	2.9	0.2	0.0	1.5	0.0	0.1	0.0	0.4	0.0
9	16/08/1999	41.0	33.5	1.0	0.1	21.2	0.0	1.1	0.0	2.3	0.4
10	26/09/1999	41.0	5.1	0.0	0.0	3.3	0.0	0.1	0.0	0.3	0.2
11	06/11/1999	40.0	24.2	2.2	3.2	11.1	0.2	0.4	0.1	1.3	1.7
12	04/12/1999	17.0	2.8	0.4	0.3	1.1	0.0	0.1	0.0	0.2	0.2
13	21/12/1999	17.0	3.9	0.3	0.2	2.1	0.0	0.1	0.0	0.1	0.4

Sample processing and diatom species examination for the Station BO-1 are described in detail in Fischer et al. (2002). In short, samples were prepared according to the methodology described in Gersonde and Zielinski (2000) and glass slides were counted following the recommendations described by Schrader and Gersonde (1978). Sediment trap samples from Station 61°S were acid-cleaned following the methodology of Romero et al. (1999, 2000). Microscopic slides were prepared following the random-settling decantation method described in Flores and Sierro (1997). The recommendations of Schrader and Gersonde (1978) were followed for counting diatom valves.

Samples from the Stations MS-4 and MS-5 were cleaned using sequential hydrogen peroxide digestions (Grigorov et al., 2014). Then, slides were prepared following the

method described by Sancetta (1992) and counted according to established conventions (Fenner, 1991; Schrader and Gersonde, 1978)

2.3 Estimation of annual diatom species contribution to total diatom valve flux

Annual relative contribution of diatom species for all stations (Table 3 and Fig. 3) were estimated calculating the integrated flux of each species for a 365-day period. Then, the annual relative contribution of each species was estimated as the ratio of the annual valve flux of a given species and the total diatom valve flux multiplied by one hundred. Due to differences in the sampling duration of the five sediment trap experiments analyzed here, some adjustments of the data sets were made to enable comparison between stations. The PZB-1 sediment trap collected particles for a total of 365 days, therefore no corrections were needed for this trap. Since the collection period for the BO-1 sediment trap was 368 days, the proportional flux of 3 days of the last cup was removed for our calculations. For Station 61ºS, the collection was shorter (309 days) than a calendar year, therefore annual estimates were calculated. These annual estimates take into consideration that the unsampled days occurred during winter when particle fluxes were low. The valve fluxes of the last winter cup were used to represent mean daily fluxes during the unobserved period (see Rigual-Hernández et al. 2015a for more details). Since MS-4 and MS-5 sediment traps sampled a total of 425 days, the data set was reduced to 365 days to enable comparison with the rest of the stations.

2.4 Environmental parameters

The monthly products of total chlorophyll-*a* concentration and contribution of major functional phytoplankton types to total chlorophyll-*a* for the five study stations for the period 1998 and 2015 were obtained from the NASA Ocean Biogeochemical model (NOBM) (accessed at https://giovanni.gsfc.nasa.gov/giovanni/). The data were extracted for a half degree area around each mooring location. Primary productivity values (mg C m^{-2} d^{-1}) for all stations were extracted from the Ocean Productivity website (accessed at www.science.oregonstate.edu/ocean.productivity/index.php/), which provides estimates of net primary productivity derived by applying the standard vertically generalized production model (VGPM; Behrenfeld and Falkowski, 1997) and the *Eppley*-VGPM productivity models to SeaWiFS chlorophyll-*a* data.

288 **2.5 Correlation analysis**

289 In order to investigate the relationship between satellite and environmental parameters
290 (i.e. sea ice cover, chlorophyll-a and primary productivity estimates) and annual
291 biogeochemical and diatom fluxes measured by the traps, a correlation matrix was
292 calculated. However, given the fact that no satellite information was available for the
293 collection period of some experiments, some assumptions had to be made for this analysis
294 as detailed next.

295 The BO-1 sediment trap was deployed before Sea-WIFS satellite began scientific
296 operations (September 1997). Moreover, the majority of the sampling intervals of MS-4
297 and MS-5 traps took place before the commencement of the Sea WIFS Chlorophyll-*a*
298 data record. Therefore, no chlorophyll-*a* data was available for the collection intervals of
299 these three stations. Nonetheless, the coefficient of variation - i.e., the standard deviation
300 of the mean divided by the mean in percentage - of chlorophyll-*a* concentration for the
301 17 years analyzed here (from 1998 until 2015) indicates little inter-annual variability for
302 the three stations: 13%, 6% and 8% for the BO-1, MS-4 and MS-5, respectively.
303 Therefore, interannual average for these stations was considered representative of the
304 sediment-trap deployment years and used in the correlation analysis. Since the sediment
305 trap deployments of stations PZB-1 and 61°S took place after 1997, the annual average
306 chlorophyll-*a* concentration for the collection year (from September to September) was
307 used in the correlation analysis.

308 Since primary productivity data is only available from 1997, a similar approach than that
309 followed for the chlorophyll-*a* concentration was followed. In this case, the coefficient of
310 variation of Eppley model for Stations BO-1, MS-4 and MS-5 was 18%, 16% and 42%,
311 respectively. For the VGMP model, the coefficient of variation for Stations BO-1, MS-4
312 and MS-5 was 21%, 20%, and 42%. Given the high interannual variability of both primary
313 productivity models, the interannual average was not considered representative of the
314 collection interval and therefore, unacceptable for the correlation analysis.

315 Sea-ice data over the sediment trap deployment locations was obtained from Pilskaln et
316 al. (2004) for Station PZB-1, Fischer et al. (2002) for Station BO-1, Rigual-Hernández et
317 al. (2015a) for Station 61°S and Grigorov et al. (2014) for Stations MS-4 and MS-5.

318 Given the low sample size (five stations) and large differences in the magnitude of
319 variables compared, correlations were considered significant at p-value < 0.1.

320

321 **3. Results**

322 **3.1 PZB-1 diatom fluxes**

323 The seasonality of diatom valve export at 1400 m at Station PFZ-1 closely
324 followed the temporal variability of total mass fluxes (Pilskaln et al., 2004) exhibiting
325 two distinct periods of enhanced diatom valve export (Fig. 2). The first and major peak
326 (up to 2.8 10^8 valves m^{-2} d^{-1}) occurred between late December 1998 and early February
327 1999, i.e. during the austral summer. Additionally, the sediment trap recorded two
328 unexpected peaks of particle export increase during the austral winter (August; up to 3.3
329 x 10^7 valves m^{-2} d^{-1}) and spring (November; up to 2.4 x 10^7 valves m^{-2} d^{-1}) when the
330 mooring location was covered by seasonal sea ice (Fig. 2).

331 A total of 60 diatom species and subspecies were identified (Table 3). At 1400 m,
332 five species accounted for 75% of the annual diatom assemblage which was co-dominated
333 by *Fragilariopsis cylindrus* (25%) and *Fragilariopsis kerguelensis* (24%), followed by
334 *Pseudo-nitzchia lineola* (10%), *Fragilariopsis curta* (9%) and *Fragilariopsis rhombica*
335 (7%).

336 Most of the diatom species fluxes at 1400 m broadly followed similar seasonal
337 trends with the highest annual fluxes during the peak of the summer bloom period (late
338 December and January) and low or negligible fluxes during the remainder of the year
339 with the exception of the two short export pulses in August and November 1999 (Fig. 2b
340 and c). Nonetheless, some important differences can be seen among species. During the
341 early period of the summer bloom (January 1999), small-sized species of the genus
342 *Fragilariopsis,* such as *F. cylindrus*, *F. pseudonana* and *F. rhombica*, *F. curta* together
343 with *Pseudo-nitzchia lineola* rapidly increased their fluxes (three-fold, five-fold, three-
344 fold, two-fold and three-fold, respectively) dominating the sinking diatom assemblage.
345 The small *Fragilariopsis* species mentioned above represented 74% of the sinking diatom
346 assemblage by the end of January (Fig. 2d). The relative abundance of this group rapidly
347 decreased in the later stages of the summer bloom, representing 34% of the assemblage
348 by late February. *Fragilariospsis kerguelensis*, that has larger and more heavily silicified
349 valves than the rest of the members of the genus *Fragilariopsis,* with major contributions
350 identified in this study, was also an important contributor to the summer bloom. However,
351 its development during the bloom differed from that of former group of species in that

352 the contribution of *F. kerguelensis* to the sinking assemblage collected by the trap
353 increased steadily during the bloom, from ~10% in January to 40% by late February.

354 The two diatom valve export pulses documented in August and November
355 exhibited a different diatom assemblage composition than that of the summer bloom. The
356 winter peak (August) was mainly caused by an increased flux of *F. kerguelensis* that
357 represented 63% of the sinking diatom assemblage, followed by *Fragilariopsis*
358 *separanda* (8%) and the two varieties of *Thalassiosira gracilis*: *T. gracilis* var. *expecta*
359 (7%) and *T. gracilis* var. *gracilis* (5%) (plotted in Figure 2 as *Thalassiosira gracilis*
360 group). The main constituent of the November peak was also *F. kerguelensis* (46%), but,
361 interestingly the secondary components of the flux were mainly composed by the small
362 *F. cylindrus* (13%) and *F. curta* (9%), *Thalassiosira lentiginosa* (7%), *F. separanda* (6%)
363 and *T. gracilis* var. *expecta* (5%).

364 **3.2 Correlation analysis**

365 The results of the correlation matrix are presented in Table 4. Total chlorophyll-*a* is
366 positively correlated with annual total diatom (r = 0.891) and small *Fragilariopsis* group
367 fluxes (r = 0.994). Both annual *F. kerguelensis* and Bio-SiO_2 fluxes are negatively
368 correlated with the annual percentage of sea-ice coverage (r = -0.960 and -0.958,
369 respectively). Lastly, annual *F. kerguelensis* flux shows a positive correlation with annual
370 Bio-SiO_2 export (r = 0.869).

371

372

373

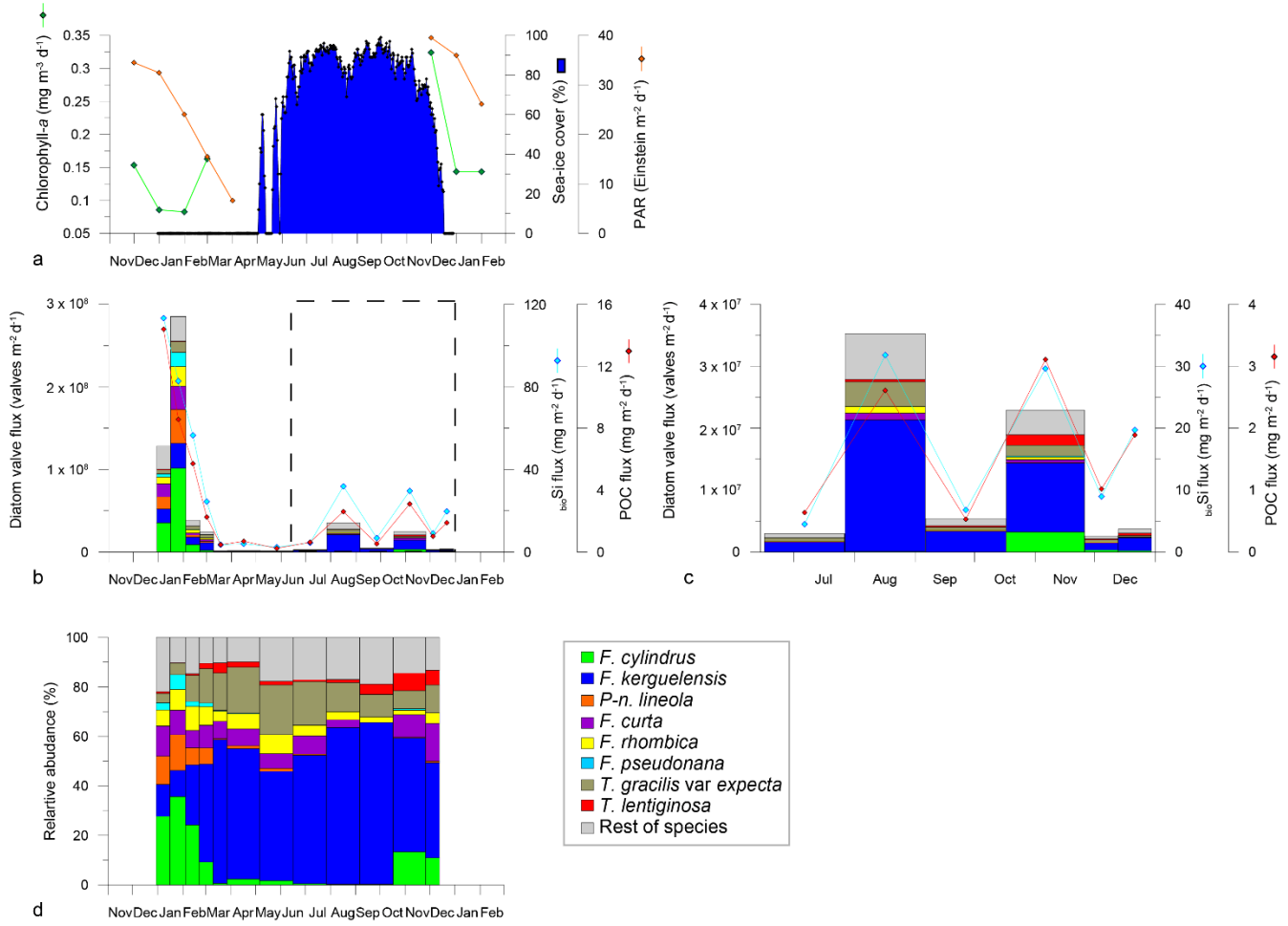

374

375 **Figure 2**. **a**. Satellite observations at PZB-1 location: monthly averaged chlorophyll-*a*
376 concentration and photosynthetically available radiation (PAR) derived from Giovanni
377 NASA website and daily percentage of sea ice cover over the trap (modified from Pilskaln
378 et al., 2004) for the period November 1998 to February 1999. **b**. Annual variability of the
379 total diatom, biogenic silica and POC fluxes at PZB-1, 1400 m (from Pilskaln et al.,
380 2004). The dashed box represents the winter period, which is shown magnified in Figure
381 2c. **c**. Annual variability of the total diatom, biogenic silica and POC fluxes plotted for
382 June-December at PZB-1, 1400 m (from Pilskaln et al., 2004). **d.** Seasonal variability of
383 the relative abundance of the main diatom taxa at PZB-1, 1400 m.

384

385 **Table 3.** List of diatom species and their annual relative contribution to total diatom flux
386 recorded from time-series sediment trap studies in the AZ of the East Antarctic Southern
387 Ocean: PZB-1 at 1400 m (this study), 61°S at 2000 m (Rigual-Hernández et al., 2015a),
388 MS-4 at 1030 m, MS-5 at 930 m (Grigorov et al., 2014) and BO1 at 450 m (Fischer et al.,

2002). Relative abundances < 0.1 are represented by an asterisk (*), whereas the absence of a taxon in a given station is represented by an empty circle (○). Only major species (nine) are shown for station BO1.

392

Species	BO1	PZB-1	61°S	MS-4	MS-5
Actinocyclus actinochilus (Ehrenberg) Simonsen		0.12	•	•	•
Actinocyclus curvatulus Janisch		•	○	•	○
Actinocyclus exiguus Fryxell et Semina		○	○	○	○
Actinocyclus octonarius Ehrenberg		○	○	•	○
Actinocyclus spp.		○	•	•	•
Alveus marinus (Grunow) Kaczmarska et Fryxell		○	○	○	○
Asteromphalus hookeri Ehrenberg		0.21	0.2	0.16	1.11
A. hyalinus Karsten		•	0.2	•	○
A. parvulus Karsten		0.34	0.2	•	•
Asteromphalus spp.		○	•	○	○
Azpeitia tabularis (Grunow) Fryxell et Sims	0.33	•	0.7	0.15	•
Banquisia belgicae (Van Heurck) Paddock		0.38	○	○	○
Chaetoceros aequatorialis var. *antarcticus* Manguin		○	•	○	○
C. atlanticus Cleve		0.95	0.2	0.19	•
C. criophilus Castracane		○	○	•	•
C. diadema Ehrenberg		○	○	○	•
C. dichaeta Ehrenberg		•	0.1	○	○
C. peruvianus Brightwell		•	○	○	○
Chaetoceros subgenus *Hyalochaete* spp.		0.49	0.2	•	0.13
Chaetoceros subgenus *Phaeoceros* spp.			0.2		
Chaetoceros resting spores		2.59	0.1	○	○
Cocconeis spp.		○	○	○	○
Corethron sp.		0.25	•	•	•
Coscinodiscus asteromphalus Ehrenberg		•	○	○	○
Cyclotella spp.		○	○	○	○
Dactyliosolen antarcticus Castracane		○	○	○	○
Diploneis bombus (Ehrenberg) Ehrenberg		○	○	○	○
Eucampia antarctica (Castracane) Mangin (summer form)		•	○	•	○
E. antarctica (Castracane) Mangin (winter form)			0.1		○
Fragilariopsis curta (Van Heurck) Hustedt	37.05	9.05	0.6	18.70	35.21
F. cylindrus (Grunow) Krieger	3.04	24.83	0.2	36.52	47.04
F. doliolus (Wallich) Medlin et Sims		○	○	○	○
F. kerguelensis (O'Meara) Hustedt	28.63	24.29	79.9	13.83	4.13
F. obliquecostata (van Heurck) Heiden		•	•	•	0.16
F. pseudonana (Hasle) Hasle		3.55	2	12.05	2.96
F. rhombica (O'Meara) Hustedt	1.47	6.67	0.9	1.43	0.79
F. ritscherii Hustedt		0.94	0.1	0.73	1.33
F. separanda Hustedt	2.72	1.76	2.1	4.53	0.18
Fragilariopsis sublinearis (Van Heurck) Heiden et Kolbe		0.57	○	○	○
F. cf. *sublineata* (Van Heurck) Heiden		○	•	○	○
Fragilariopsis vanheurckii (Peragallo) Hustedt		0.26	○	○	○
Fragilariopsis spp.		○	○	○	○
Guinardia spp.		○	○	○	•
Gyrosigma spp.		○	○	○	○
Haslea trompii (Cleve) Simonsen		0.16	•	○	○
Hemidiscus cuneiformis Wallich		○	○	○	○
Manguinea spp.		•	○	○	○
Membraneis spp.		0.33	○	○	○
Navicula directa (Smith) Ralfs in Pritchard		0.23	0.3	○	○
Navicula spp.		•	○	0.55	0.55
Nitzschia bicapitata Cleve		○	○	○	○
N. braarudii (Hasle)		○	○	○	○
N. kolaczeckii Grunow		○	○	○	○
N. sicula (Castracane) Hustedt var. *bicuneata* Grunow		○	0.1	○	○
N. sicula (Castracane) Hustedt var. *rostrata* Hustedt		0.10	○	○	○
Nitzschia spp.		○	○	○	○
Paralia spp.		0.04	○	○	○
Pleurosigma spp.		○	•	0.01	○
Pleurosigma directum		0.03	○	○	○
Porosira pseudodenticulata (Hustedt) Jousé		○	•	○	○
Proboscia alata (Brightwell) Sundström		•	○	○	○
P. inermis (Castracane) Jordan et Ligowski		•	○	○	○

Species	BO1	PZB-1	61°S	MS-4	MS-5
P. truncata (G.Karsten) Nöthig et Ligowski		•	○	○	○
Proboscia spp.		•	○	○	○
Psammodiction panduriforme (Gregory) Mann		○	○	○	○
Pseudo-nitzschia cf. *lineola*		○	0.4	○	○
P-n. lineola (Cleve) Hasle		9.57	○	2.30	3.18
P-n. turgiduloides (Hasle) Hasle		1.58	○	○	○
P-n. prolongatoides (Hasle) Hasle		0.22	○	○	○
P-n. heimii Manguin		○	•	○	○
Pseudo-nitzschia spp.		•	0.1	○	0.13
Rhizosolenia antennata (Ehrenberg) Brown f. *antennata*		•	○	○	○
R. antennata (Ehrenberg) Brown f. *semispina* Sundström		0.70	○	○	○
R. bergonii Peragallo		○	○	○	○
Rhizosolenia cf. *costata*		○	○	○	○
Rhizosolenia cf. chunii		0.23	○	○	○
R. curvata Zacharias		○	○	○	○
R. polydactyla Castracane f. *polydactyla*		○	○	○	○
R. polydactyla Castracane f. *squamosa*		•	○	○	○
R. simplex Karsten		○	○	•	○
R. sima Castracane		○	○	○	•
R. styliformis Brightwell		○	○	•	○
Rhizosolenia sp. f. 1A *sensu* Armand et Zielinski		•	•	○	○
Rhizosolenia spp.		○	0.1	○	○
Roperia tesselata (Roper) Grunow		○	○	○	○
Stellarima stellaris (Roper) Hasle et Sims		○	○	○	○
Synedropsis sp.		•	○	○	○
Thalassionema nitzschioides var. *capitulata* (Castracane) Moreno-Ruiz		○	0.1	○	○
T. nitzschioides var. *lanceolata* (Grunow) Pergallo et Pergallo		○	0.1	•	○
T. nitzschioides var. *parvum* Moreno-Ruiz		○	○	○	○
T. nitzschioides var. 1 *sensu* Zielinski et Gersonde	3.45	○	○	•	0.16
Thalassiosira antarctica Comber		•	○	•	0.09
T. decipiens (Grunow ex Van Heurck) Jørgensen		○	○	○	0.17
T. eccentrica (Ehrenberg) Cleve		○	0.2	○	○
T. ferelineata Hasle et Fryxell		○	○	○	○
T. gracilis var. *expecta* (Van Landingham) Fryxell et Hasle		5.20	0.4	7.09	○
T. gracilis var. *gracilis* (Karsten) Hustedt		1.40	3.6		○
T. gracilis group		○	4.1	○	1.67
T. gravida Cleve	6.97	0.43	•	0.14	0.12
T. lentiginosa (Janisch) Fryxell	2.79	1.26	5	0.81	0.27
T. leptopus (Grunow ex Van Heurck) Hasle et Fryxell		○	•	○	○
T. lineata Jousé		○	○	○	○
T. maculata Fryxell et Johans		○	•	○	○
T. oestrupii (Ostenfeld) Hasle var. *oestrupii* Fryxell et Hasle		•	•	0.13	0.02
T. oestrupii (Ostenfeld) Hasle var. *venrickae* Fryxell et Hasle			○		○
T. oliveriana (O'Meara) Makarova et Nikolaev		•	0.7	○	0.07
T. symmetrica Fryxell et Hasle		○	○	○	○
T. trifulta Fryxell		0.11	○	○	○
T. tumida (Janisch) Hasle		•	0.1	○	○
Thalassiosira sp. 1		○	•	○	○
Thalassiosira sp. 2		○	○	○	○
Thalassiosira sp. 3		○	○	○	○
Thalassiosira eccentric group		○	○	○	○
Thalassiosira. linear group		○	0.1	○	○
T. trifulta group		○	○	○	○
Thalassiosira spp. < 20 µm		○	0.4	•	○
Thalassiosira spp. > 20 µm		○	•		○
Thalassiothrix antarctica Schimper ex Karsten		○	0.2	0.20	0.23
Thalassiothrix longissima + *antarctica*		0.46	○	○	○
Trachyneis aspera (Ehrenberg) Cleve		○	○	○	○
Trichotoxon reinboldii (Van Heurck) Reid et Round		•	○	•	0.10
Tropidoneis group		○	•	○	○
Other centrics		•	•	○	○
Other pennates		•	0.1	○	○

393

Table 4. Correlation matrix (r) for the main environmental parameters, diatom and biogeochemical fluxes measured at the study stations. Correlation in red are significant at $p < 0.1$.

	Total Chl-*a* concentration	Sea ice cover	Total diatom flux	*F. kerguelensis* flux	Small *Fragilariopsis* group flux	Biogenic Silica flux	POC flux	POC flux normalized at 2000m
Total Chl-*a* concentration	1.000 p= ---							
Sea ice cover	-0.029 p=.964	1.000 p= ---						
Total diatom flux	0.891 p=.043	-0.433 p=.467	1.000 p= ---					
F. kerguelensis flux	0.218 p=.724	-0.960 p=.010	0.588 p=.297	1.000 p= ---				
Small *Fragilariopsis* group flux	0.944 p=.016	-0.235 p=.703	0.977 p=.004	0.409 p=.494	1.000 p= ---			
Biogenic Silica flux	-0.056 p=.929	-0.958 p=.010	0.379 p=.529	0.869 p=.056	0.199 p=.749	1.000 p= ---		
POC flux	0.236 p=.702	-0.055 p=.930	0.381 p=.527	-0.008 p=.990	0.433 p=.466	0.297 p=.627	1.000 p= ---	
POC flux normalized at 2000m	0.419 p=.482	-0.637 p=.247	0.730 p=.162	0.787 p=.114	0.650 p=.236	0.588 p=.297	0.244 p=.692	1.000 p= ---

5. Discussion

5.1 Seasonal drivers of diatom community development and valve fluxes at PZB-1

Increasing irradiance and air temperature in springtime, along with sea ice melting processes, resulted in a moderate increase in the algal biomass, as inferred from the satellite derived chlorophyll-*a* concentration (Fig. 2a). As sea ice melts, it releases nutrients and dust particles intercepted during ice formation that stimulate phytoplankton growth (Sedwick and DiTullio, 1997; van der Merwe et al., 2011). Partitioning of the chlorophyll-*a* signal between major phytoplankton groups by the NASA Ocean Biogeochemical Model (NOBM) suggests that diatoms largely dominate the phytoplankton communities at the study station, accounting for > 99% of the chlorophyll-*a* production (Fig. 4). The high contribution of diatoms to the total chlorophyll-*a* concentration at PZB-1 station most likely represents an overestimation of their real abundance as a result of the NOBM limitations (Hirata et al., 2011; Rousseaux and Gregg, 2012). Nonetheless, these results reinforce the idea that diatoms dominate the phytoplankton assemblages in the PZB-1 region and are consistent *in situ* observations of phytoplankton community composition in pelagic Southern Ocean systems under the influence of recent sea ice melt (e.g. DiTullio and Smith, 1996; Kang et al., 2001) where mix layers are often shallow and stratified. These conditions favor the development of

418 diatoms over *Phaeocystis antarctica*, a colonial haptophyte known to regularly develop
419 large blooms in seasonal ice zones and coastal Antarctic waters with deep mixed layer
420 due to its ability to sustain near-maximal photosynthetic rates at much lower solar
421 irradiance levels than do diatoms (Arrigo et al., 1999; Kropuenske et al., 2010; Mills et
422 al., 2010).

423 Diatom export at PZB-1 1400 m basically followed the seasonal trend of
424 chlorophyll-*a* concentrations in the surface layer as documented by monthly composites
425 of SeaWifs data from the study region and summarized in Pilskaln et al. (2004).

426 About two thirds of the annual diatom valve export occurred during a short
427 interval of 36 days (Dec. 30 - Feb. 4; Pilskaln et al., 2004). The pronounced diatom valve
428 export was coupled with a strong pulse of organic carbon and biogenic silica that
429 accounted for about half of the annual carbon and silica export at 1400 m(Pilskaln et al.,
430 2004) . This pronounced and short-lived pulse of diatom production and export is a
431 common feature in the circumpolar AZ (Fischer et al., 2002; Grigorov et al., 2014;
432 Rigual-Hernández et al., 2015a) and likely the primary driver of atmospheric CO_2
433 sequestration in this zonal region of the Southern Ocean.

434

435 **5.2 Diatom species succession at 1400 m at PZB-1**

436 Ice melting processes in SIZ systems have been suggested to seed the surface
437 waters with phytoplankton cells accumulated in the sea ice that grow in the stable surface
438 waters after their release (Mangoni et al., 2009; Riaux-Gobin et al., 2011). This situation
439 seems to be the case for the PFZ-1 system as suggested by the large contribution of
440 *Fragilariopsis cylindrus* and *Fragilariopsis curta* to the summer bloom, as both species
441 have been reported to thrive abundantly in the waters adjacent to the ice and in the ice
442 itself (Kang and Fryxell, 1992; Scott et al., 1994; Leventer, 1998; Kang et al., 2001;
443 Riaux-Gobin et al., 2011). Despite the large contribution of sea-ice affiliated species to
444 the annual bloom, the strong contribution of open ocean species (mainly represented by
445 *F. kerguelensis*, *Pseudo-nitzschia lineola* and *Thalassiosira gracilis* group) also suggests
446 a significant input of pelagic phytoplankton communities over station PZB-1.

447 Regardless of their sea-ice preference, most of the diatom species contributing to
448 the peak in valve flux at PZB-1 are characterized by a boom-and-bust life strategy (i.e. r-

449 selected strategists). This group of diatoms, mainly represented by small *Fragilariopsis*
450 species and *Pseudo-nitzschia lineola*, posses a suite of functional traits such as small cell
451 sizes, weakly silicified frustules and high rates of nutrient acquisition, growth and
452 reproduction (Assmy et al., 2007; Durkin et al., 2012) that favor their rapid development
453 at the initial stages of the diatom bloom (Quéguiner, 2013). The high abundance of the
454 needle-shaped *Pseudo-nitzchia lineola* in the PZB-1 traps is consistent with previous
455 studies that reported species of this genus as one of the major components of diatom
456 blooms in the pelagic waters of the ACC (Hasle and Syvertsen, 1997; Kopczynska et al.,
457 2001; Smetacek et al., 2002; Assmy et al., 2007). Moreover, *Pseudo-nitzchia* species
458 represent important vectors of both carbon and silica flux to the deep ocean since they
459 have been reported to reach meso- and bathypelagic depths of the water column with a
460 significant fraction of their cellular organic content intact (Smetacek et al., 2012;
461 Rembauville et al., 2014).

462 The three- to four-fold increase in *F. cylindrus*, *F. rhombica* and *F. pseudonana*
463 fluxes during the growth phase of the bloom (i.e. from cup 1 to 2) and rapid decline in
464 their relative contribution from cup 3 are in contrast with the less pronounced two-fold
465 flux increase of *F. kerguelensis* but gradual increase in its relative abundance from mid-
466 summer throughout autumn (Fig. 2). The distinct seasonal trend of *F. kerguelensis* flux
467 suggests an ecological strategy different than the rest of the main components of the
468 diatom bloom. *Fragilariopsis kerguelensis* life strategy has been described as "persistent"
469 by Assmy et al. (2013) based on the lower growth rates of this species compared to that
470 of other major components of the bloom and its strong mechanical protection (Hamm et
471 al., 2003) against the heavy zooplankton grazing in the ACC (Pollard et al., 2002;
472 McLeod et al., 2010).

473 The two small flux peaks measured by the traps occurring in August and October-
474 November were unexpected given the fact that sea ice coverage started to build-up in
475 May, covering the mooring location completely from June until November (Fig. 2a).
476 Based on the large contribution of *F. kerguelensis* in the first peak, Pilskaln et al. (2004)
477 attributed the August pulse to an injection of material advected laterally into the trap from
478 an area of open, ice-free water. Indeed, NOAA Advanced Very High Resolution
479 Radiometer (AVHRR) imagery suggests the incursion of winds from mid-latitudes over
480 the study region between the 15th and 19th of August (supplementary Figure 1a). These
481 winds could have helped to propel warmer surface water masses towards the Station PZB-

1. Additionally, SSM/I ice concentration images from the National Snow and Ice Data Center (supplementary Figure 1b) support this interpretation indicating the reduction of sea ice concentration over the Station PZB-1 during a period of 12 days in mid-August, probably as a result of the southward injection of warmer waters from this major atmospheric event. This idea is further supported by the rest of the diatom assemblage collected by the trap that is mainly composed of open ocean species, such as the *Thalassiosira gracilis* group (12%), considered a cool open ocean taxon with peak abundances within the maximum winter sea-ice edge (Crosta et al., 2005), and *Fragilariopsis separanda* (8%) reported to display a similar distribution to *F. kerguelensis* in the Indian Ocean (Mohan et al., 2006). Based on this evidence, we speculate that first winter export peak could have been the result of the transport of an ice-free water masses by a major atmospheric event over the mooring location.

The secondary export pulse in all components measured in late October through late November likely had a different origin than the August peak. The onset of the sea-ice retreat around the PZB-1 trap in November together with the increase in light levels resulted in the initiation of the phytoplankton bloom as suggested by the increase in chlorophyll-*a* concentration (Fig. 2). The development of a diatom bloom under sea-ice conditions is consistent with previous investigations that have reported large under-ice phytoplankton blooms in polar environments (e.g. Arrigo et al., 2012; Lowry et al., 2018; Nomura et al., 2018) The high contribution of the sea-ice affiliated species *F. cylindrus* and *F. curta* (13% and 9%, respectively) during the November supports the idea of an early initiation of the phytoplankton bloom triggered by the receding sea ice as previously suggested by Pilskaln et al. (2004).

5.3 Distribution of diatom species across different sectors of the Antarctic Zone

Diatom assemblages at all stations were overwhelmingly dominated by species of the genus *Fragilariopsis* with secondary contribution by *Pseudo-nitzschia lineola*/cf. *lineola* (Fig. 3). Despite the fact that these species are often important contributors to the living diatom assemblages in the surface layer in the AZ, they are most likely overrepresented in the sediment traps due to selective dissolution in the upper water column and mechanical breakage by zooplankton of weakly silicified species that can

cause profound modifications in the original diatom assemblage (McMinn, 1995; Jordan and Stickley, 2010; Rigual-Hernández et al., 2016). The variations in the composition of the diatom sinking assemblages across the stations seem to be largely determined by the influence of sea ice cover, a critical factor determining the distribution of diatom assemblages in the modern sediments of the Southern Ocean (Zielinski and Gersonde, 1997; Armand et al., 2005). Maximum annual fluxes and relative contribution of *F. kerguelensis* are observed at Station 61°S, the only station not affected by sea ice, while minimum fluxes and relative contribution of this species are displayed at the MS-5 station, characterized by the highest annual sea ice cover of all stations (Figs. 3 and 4). The negative effect of sea ice on *F. kerguelensis* distribution is supported by the negative and significant correlation between both variables (Table 4). Our observation on sediment trap fluxes is consistent with many previous reports on diatom assemblages from Southern Ocean sediments that described high abundance of this species as a proxy for the iron limited waters of the ACC (Burckle and Cirilli, 1987; Taylor et al., 1997; Crosta et al., 2005; Pike et al., 2008, among others).

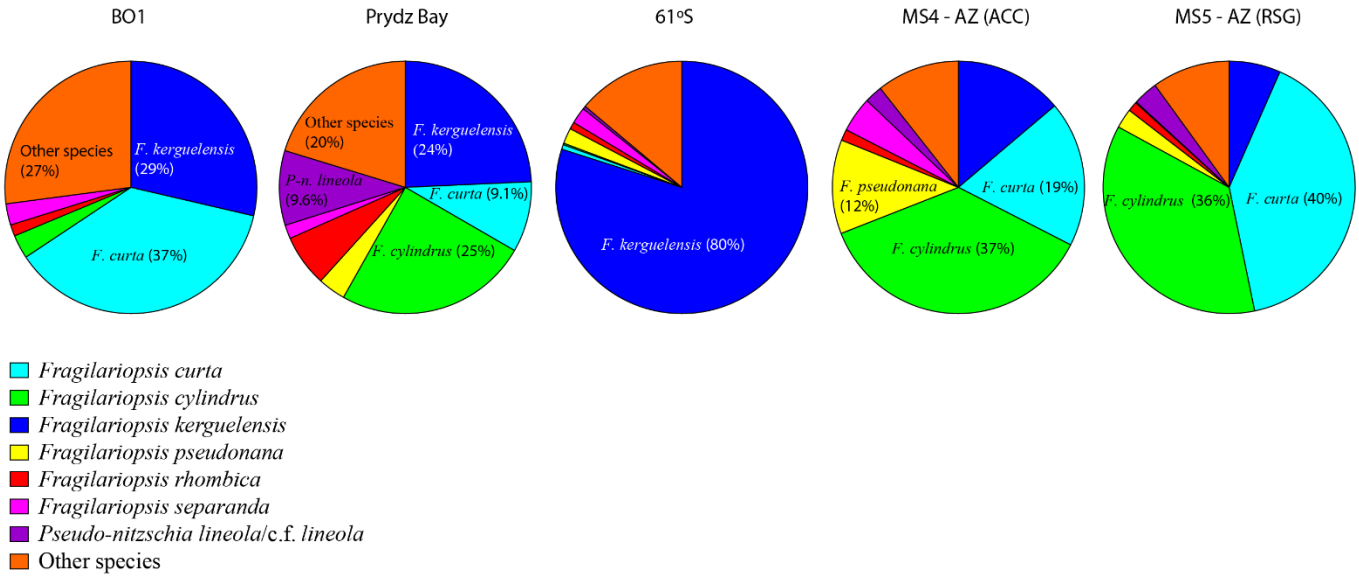

Figure 3. Annual relative contribution of the major diatom species recorded in AZ sediment traps of the East Antarctic Southern Ocean.

In contrast, *Fragilariopsis curta* and *Fragilariopsis cylindrus* display peak relative abundances at those stations under the seasonal influence of sea ice cover (Fig. 3 and 4). The sea-ice affinity of these species is consistent with their biogeographical distribution in the modern Southern Ocean where they are often found in high numbers in the surface waters near the marginal ice-edge zones (e.g. Kang and Fryxell, 1992; Kang et al., 2001), as part of sea ice communities (Scott et al., 1994; Ugalde et al., 2016) and in the surface sediments in regions under the influence of sea ice (Zielinski and Gersonde, 1997; Armand et al., 2005). *Fragilariopsis pseudonana* exhibited its highest relative contribution at MS-4, a station also characterized by peak diatom biomass accumulation and diatom valve fluxes of all stations. Although *F. pseudonana* is often reported as an important contributor to the phytoplankton communities in the Southern Ocean waters (Kang and Lee, 1995; Villafañe et al., 1995; Kopczynska et al., 2001; Kopczyńska et al., 2007; Cefarelli et al., 2010), it is often not preserved in the sedimentary record (Grigorov et al., 2014) most likely due to its weak silicification. High diatom biomass accumulation is known to facilitate mass aggregation, increase sinking rates and promote the deep-water delivery of diatom frustules (Alldredge and Goltschalk, 1989; Passow et al., 2003). Therefore, it is possible that the relatively high abundance of *F. pseudonana* at MS-4 trap was due to high diatom biomass accumulation in the upper surface waters with subsequent aggregation and sinking, thus increasing the probability of *F. pseudonana* transiting through the mixed layer and reaching the sediment trap depth intact. Lastly, it is important to note that annual fluxes of the small *Fragilariopsis* species group - composed by *F. curta*, *F. cylindrus, F. rhombica* and *F. separanda* – display a robust and significant correlation with total chlorophyll-*a* concentration ($r = 0.944$, $p = 0.016$) which highlights the potential of this group species as a proxy of high algal biomass accumulation in Southern Ocean paleorecords. Nonetheless, we acknowledge that caution should be taken in the interpretation of the results of our correlation matrix because low sample size of the current study limits ability to make strong statistical statements.

The genus *Pseudo-nitzchia* is cosmopolitan in the Southern Ocean waters but their frustules are often not represented in the sedimentary record presumably due to dissolution at the sediment-water interface and in the uppermost bottom sediments (Rigual-Hernández et al., 2016). Nonetheless, despite their poor preservation *Pseudo-nitzchia* species have been reported in the surface sediments of the Pacific and Prydz Bay

sectors of the AZ (Taylor et al., 1997; Grigorov et al., 2014) which coincide with stations displaying peak relative abundance of species of this genus (i.e. MS-4, MS-5 and PZB-1; Fig. 3).

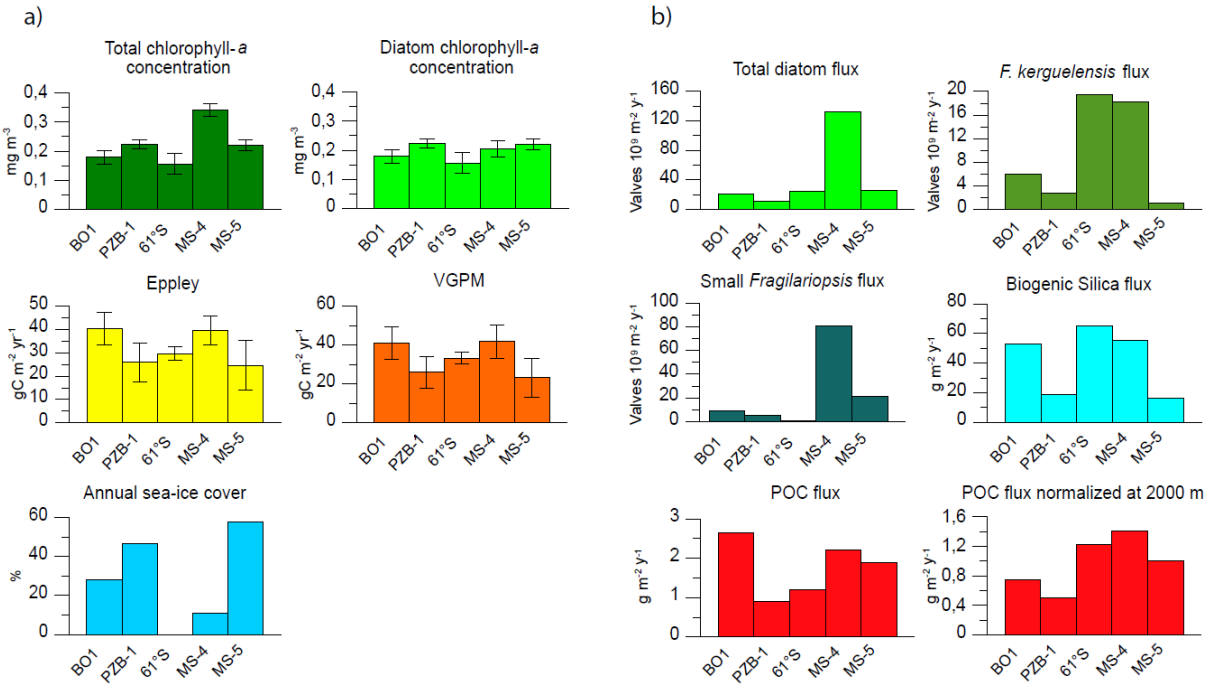

Figure 4. Antarctic Zone station comparisons: BO1, PZB-1, 61°S, MS-4 and MS-5. **a.** Annual average total chlorophyll-*a* concentration, diatom chlorophyll-*a* concentration, two model estimates of primary productivity (VGPM and Eppley), and percent sea ice cover for the 5 stations obtained from the NOBM model**. b.** Annual fluxes of total diatom valves, major diatom species (*F. kerguelensis* and small *Fragilariospsis* group*), biogenic silicate, POC at sediment trap depths (BO-1, 450 m; PZB-1, 1400 m; 61°S, 2000 m; MS-4, 1031 m; MS-5, 937) and 2000 m-normalized POC (after Honjo et al., 2008). *Small *Fragilariopsis* group includes *F. curta*, *F. cylindrus*, *F. rhombica* and *F. separanda*.

5.4 Variations in annual biogenic particle export between sectors of the Antarctic Zone particle composition and their relationship with diatom assemblages

All the sediment traps discussed in this study (Table 1) were deployed far below the ventilation depths of the AZ (approximately 100 m; Trull et al., 2001), thereby providing a direct measurement of the annual extraction of carbon from the atmosphere by biological processes. In order to objectively compare the AZ trap data sets from different mesopelagic depths, annual POC fluxes were normalized to 2 km after the Honjo et al. (2008) study using the Berelson (2001) empirical POC flux reduction formula with a power constant of 0.87 (Figure 4). Taking into account that the majority of biogenic silicate dissolution occurs in the upper water column with minimal dissolution loss in the mesopelagic zone (Ragueneau et al., 2002; Rigual-Hernández et al., 2015a; Rigual-Hernández et al., 2016), diatom valve and biogenic silicate fluxes were not normalized.

Annual Bio-SiO_2 fluxes at mesopelagic depths at the five AZ stations were between 2 to 9 times higher than the mean opal export fluxes at the 2 km mesopelagic/bathypelagic boundary in the global ocean of 6.9 g SiO_2 m^{-2} yr^{-1} reported in Honjo et al. (2008). The peak Bio-SiO_2 fluxes measured in the Australian and New Zealand sectors of the AZ (i.e. 61°S and MS-4 stations, respectively) represent two of the largest annual opal exports ever measured in the global ocean (Honjo et al., 2008; Rigual-Hernández et al., 2015b) rivalled only by the North Pacific Boreal Gyres (48 g SiO_2 m^{-2} yr^{-1} at the Aleutian-Bering Station; Takahashi et al., 2000). The large Bio-SiO_2 export fluxes in the pelagic AZ are linked to the vicinity of the Antarctic Divergence where the upwelling of deep nutrient-rich waters (Pollard et al., 2006) enhance diatom growth and facilitate opal preservation in underlying sediments. Given the fact that diatoms are by far the main biogenic silica exporters in the AZ waters (Grigorov et al., 2014; Rigual-Hernández et al., 2015a), the weak and non-significant correlation between annual diatom valve and Bio-SiO_2 fluxes ($r = 0.379$, $p = 0.529$) is somewhat surprising. This poor correlation is most likely due to the large differences in biogenic silica (BSi) content per cell of the dominant diatom species at each location. Particularly important is the pronounced difference in BSi content between the different species of the genus *Fragilariopsis* that dominated the sinking assemblages at all stations. While diatom assemblages at Station 61°S were mainly composed of the relatively large and heavily silicified *Fragilariopsis kerguelensis* (80% of the annual diatom export), MS-4 and MS-5 assemblages were dominated by *Fragilariopsis curta* (19% and 35%, respectively) and *Fragilariopsis cylindrus* (37% and 47% at both stations) characterized by smaller cell sizes and weak silicification. Indeed, when comparing Bio-SiO_2 and valve fluxes of *F.*

620 *kerguelensis* alone, they yield a much stronger correlation (r = 0.869, p = 0.056)
621 suggesting that *F. kerguelensis* is the main vector of BSi to the deep ocean at all the study
622 stations regardless its relative contribution to the total assemblage. This result highlights,
623 once again, the critical role of *F. kerguelensis* in the silica cycle of the Southern Ocean,
624 particularly in the AZ where it is the main species responsible for the formation of the
625 silica-rich deposits that encircle Antarctica between the winter sea ice edge and the
626 Antarctic Polar Front (Burckle and Cirilli, 1987; Crosta et al., 2005).

627 POC export fluxes at 2000 m varied across the AZ stations with values about two-fold
628 lower in the Eastern Atlantic (Station BO 1) and offshore Prydz Bay (Station PZB-1) than
629 to those observed in the Western Pacific sector, where station MS-4 displayed the highest
630 POC fluxes of all stations (1.4 g C m^{-2} yr^{-1}; Fig. 4). The high POC export fluxes at the
631 MS-4 coincide with the highest chlorophyll-*a* concentration and primary productivity
632 estimates of all stations. These results are in agreement with Arrigo et al. (2008) who
633 described the Ross Sea sector as the most productive region of the Southern Ocean and
634 with Nelson et al. (2002) who documented high algal accumulation and high POC export
635 fluxes around the MS-4 deployment site. The temporal variations between the POC, Bio-
636 SiO_2 and diatom fluxes were strongly correlated at all stations (Fischer et al., 2002;
637 Grigorov et al., 2014; Rigual-Hernández et al., 2015a and this study). However, when the
638 magnitude of the annual fluxes of these three parameters is compared (Fig. 4), the
639 correlation between them is not significant (Table 4), indicating that the amount of
640 organic carbon sequestered to the ocean interior across the AZ is not directly proportional
641 to the amount of opal or diatom cells sinking out the mixed layer. These results suggest
642 that although diatoms represent a major vector of organic carbon to the ocean interior in
643 the AZ, other factors aside from the ballast effect of biogenic silica and diatom abundance
644 must play a major role in the efficiency by which POC is transported to the deep sea in
645 AZ ecosystems. Many factors including ecosystem structure and composition, as well as
646 physical (e.g. insolation, water column stability, annual sea ice cover, etc.) and chemical
647 parameters (e.g. availability of macro- and micronutrients, etc.) are known to influence
648 the magnitude and composition of the particles sinking to the deep ocean (e.g. Wassmann,
649 1998; Honjo et al., 2008; Ebersbach et al., 2011; Laurenceau-Cornec et al., 2015). Among
650 them, the makeup of the diatom community (i.e., diatom floristics) has been suggested to
651 be one of the main factors responsible for setting the different degree of coupling between
652 carbon and silicon in the particles sinking in the AZ (Assmy et al., 2013; Boyd, 2013).

653 The poor correlation between diatom valve and POC fluxes recorded in the traps is known
654 to be largely determined by the pronounced differences in organic carbon content between
655 diatom species and differences in the full cell: empty cell ratios of the diatom cells
656 reaching the trap depths. Indeed, previous sediment trap studies in other Southern Ocean
657 settings have demonstrated that the ratio of full to empty diatoms cells largely vary
658 between species, representing a first-order control in the BSi : POC export stoichiometry
659 of a given ecosystem. For example, Salter et al. (2012), Rembauville et al. (2014) and
660 Rembauville et al. (2016) highlighted the important role of resting stages from *Eucampia*
661 *antarctica* var. *antarctica*, *Chaetoceros* and *Thalassiosira antarctica* in the export of
662 organic carbon from the surface to the deep ocean. Moreover, organisms of higher trophic
663 levels are known to exert a significant influence in the efficiency of the transfer of organic
664 matter from the euphotic zone into the deep layers of the water column either through the
665 formation of faecal pellets (e.g. Lampitt et al., 2009; Ebersbach et al., 2011; Rembauville
666 et al., 2014; Manno et al., 2015; Belcher et al., 2017) or by vertical migrations (e.g.
667 Jackson and Burd, 2001; Davison et al., 2013). Thus, different zooplankton composition
668 at each of the studied stations may also account for part of the POC variability export
669 across regions of the AZ.

670 Lastly, the importance of heterotrophic bacteria in determining the degradation depths of
671 POC is becoming increasingly evident. A recent study by Edwards et al. (2015)
672 demonstrated how carbon-rich diatom aggregates sinking out the surface layer can be hot
673 spots for production of polyunsaturated aldehydes (PUAs), highly bioactive molecules
674 that can stimulate bacteria respiration at adequate concentrations. The stimulation of the
675 metabolism of the heterotrophic bacteria by the PUAs results in the faster
676 remineralization of phytoplankton-derived sinking organic matter leading to the shoaling
677 of remineralization depths of carbon and other nutrients. Taking into that the diatom
678 species dominating each of the sectors of the AZ exhibit significantly different life
679 strategies and metabolisms, variations in PUAs production between different polar
680 diatom species is likely, and therefore it could potentially play an important role in the
681 export efficiency in diatom dominated ecosystems such as the ones compared here.

682

683 **Conclusions**

684

In this study we analyzed diatom floristics, POC, Bio-SiO_2 fluxes, and environmental parameters across key regions of the AZ. In the first part of the study we documented the seasonal variability of diatom species and its relationship with biogeochemical fluxes intercepted by a sediment trap over a year in the offshore waters of Prydz Bay. A short and pronounced diatom valve export period during the summer season co-occurred with the highest annual POC fluxes at the PZB-1 station, suggesting that diatoms represent the main organic carbon vectors to ocean interior in this region. Two peaks of enhanced export were recorded during winter and autumn, a period characterized by extensive sea ice cover. Taxonomic analysis of the diatom assemblages of these two export events suggest different origins of the materials collected by the trap: the August peak seems to be caused by lateral advection event while the November maximum seems to be the result of the initiation of the sea-ice retreat and consequent onset of the spring phytoplankton bloom.

In the second part of the study, five sediment trap experiments reporting diatom assemblage composition and biogeochemical fluxes conducted in different regions of the AZ were compared. The relative abundance of *F. kerguelensis* at all the study stations seems to be largely influenced by the presence of sea ice, with maximum abundance of this species in the only station not affected by sea ice and minima in the southernmost site of the Ross Sea sector, characterized by the highest annual sea ice cover of all stations. Annual fluxes of the small *Fragilariopsis* species group exhibited a strong and significant correlation with total chlorophyll-*a* concentration across stations. This observation highlights the potential of these species as a proxy of high algal biomass accumulation in Southern Ocean paleorecords. Despite the fact that diatoms are the main Bio-SiO_2 producer at all stations, the annual biogenic silica and diatom valve export fluxes did not covary across sites. This is most likely due to the pronounced differences in biogenic silica content per cell of the dominant diatom species at each study station. Interestingly, annual Bio-SiO_2 and *F. kerguelensis* fluxes alone exhibited a much stronger correlation which underscores, once again, the major role of this species for selective silicon export into the ocean interior of the AZ.

Supplementary material

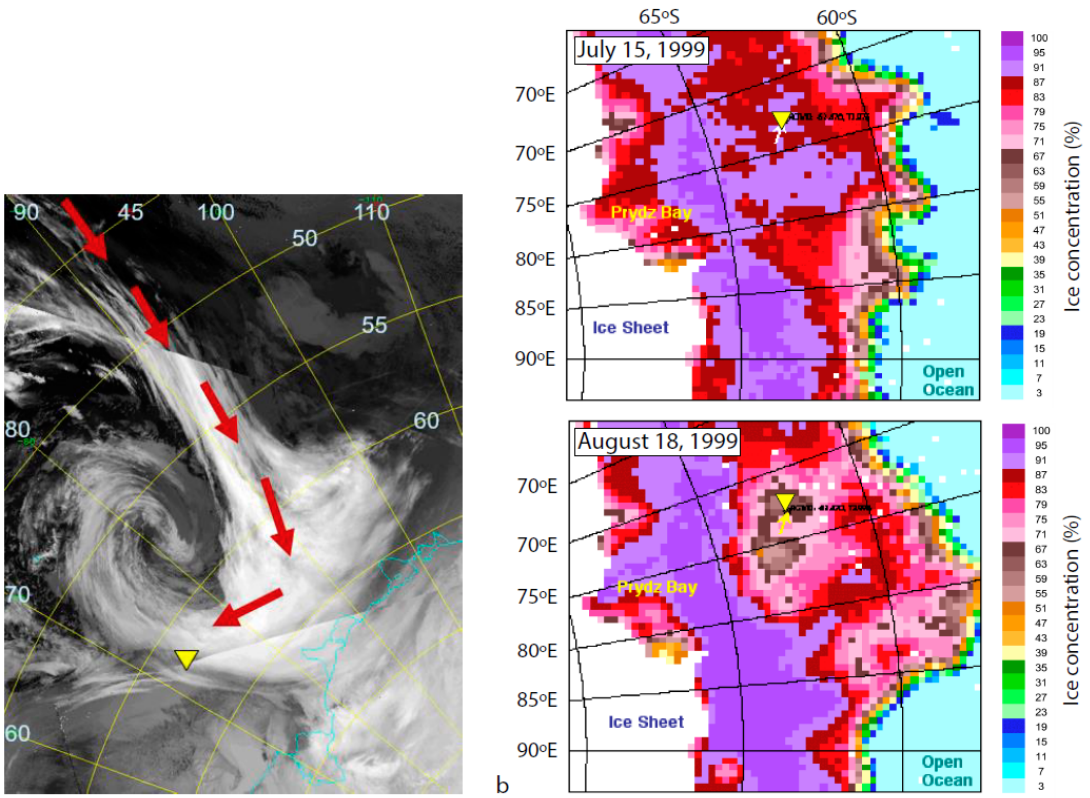

715

716 **Supplementary Figure 1: a**. NOAA Advanced Very High Resolution Radiometer
717 Channel 4 mosaic (thermal IR) between 15th -19th of August 1999, 4 km resolution for
718 the study region. **b**. Daily ice concentration maps for the study region during July 15,
719 1999 (typical winter conditions) and August 18, 1999 (showing small open water areas
720 in the sea-ice around the sediment trap location). Yellow triangle shows the position of
721 the sediment trap PZB-1.

722 **Supplement II.** Diatom species flux data of PZB-1 (excel file).

723 **Acknowledgements**:

724 We are grateful to the scientific members of CHINARE 15/16, as well as the many people
725 of the Australian Antarctic Division and at the Antarctic CRC (Hobart, Tasmania) who
726 provided much of the technical assistance in numerous phases of the project. We also
727 thank Captain Shao Yuan of the Xue Long and his crew for assistance in the PZB-1
728 mooring work. This project was funded by NSF OPP-9726186 to C. Pilskaln and F. Chai.
729 Additional thanks are conveyed to Dr J.J-Pichon (University of Bordeaux) and Dr I.
730 Grigorov (Uni South Hampton) for diatom discussions. We would like to thank three
731 anonymous reviewers for their valuable comments that helped to improve the manuscript.

732

733 **References**

734 Alvain, S., Moulin, C., Dandonneau, Y., Loisel, H., 2008. Seasonal distribution and
735 succession of dominant phytoplankton groups in the global ocean: A satellite view.
736 Global Biogeochemical Cycles 22, GB3001.

737 Alldredge, A.L., Goltschalk, C.G., 1989. Direct observations of the mass flocculation of
738 diatom blooms: characteristics, settling velocities and formation of diatom aggregates.
739 Deep-Sea Research 36, 159-171.

740 Antoine, D., André, J.-M., Morel, A., 1996. Oceanic primary production: 2. Estimation
741 at global scale from satellite (Coastal Zone Color Scanner) chlorophyll. Global
742 Biogeochemical Cycles 10, 57-69.

743 Armand, L.K., Crosta, X., Romero, O., Pichon, J.-J., 2005. The biogeography of major
744 diatom taxa in Southern Ocean sediments: 1. Sea ice related species. Palaeogeography,
745 Palaeoclimatology, Palaeoecology 223, 93-126.

746 Arrigo, K.R., Perovich, D.K., Pickart, R.S., Brown, Z.W., van Dijken, G.L., Lowry, K.E.,
747 Mills, M.M., Palmer, M.A., Balch, W.M., Bahr, F., Bates, N.R., Benitez-Nelson, C.,
748 Bowler, B., Brownlee, E., Ehn, J.K., Frey, K.E., Garley, R., Laney, S.R., Lubelczyk, L.,
749 Mathis, J., Matsuoka, A., Mitchell, B.G., Moore, G.W.K., Ortega-Retuerta, E., Pal, S.,
750 Polashenski, C.M., Reynolds, R.A., Schieber, B., Sosik, H.M., Stephens, M., Swift, J.H.,
751 2012. Massive Phytoplankton Blooms Under Arctic Sea Ice. Science 336, 1408-1408.

752 Arrigo, K.R., Robinson, D.H., Worthen, D.L., Dunbar, R.B., DiTullio, G.R., VanWoert,
753 M., Lizotte, M.P., 1999. Phytoplankton Community Structure and the Drawdown of
754 Nutrients and CO2 in the Southern Ocean. Science 283, 365-367.

755 Arrigo, K.R., van Dijken, G.L., Bushinsky, S., 2008. Primary production in the Southern
756 Ocean, 1997–2006. Journal of Geophysical Research: Oceans 113, C08004.

757 Assmy, P., Henjes, J., Klaas, C., Smetacek, V., 2007. Mechanisms determining species
758 dominance in a phytoplankton bloom induced by the iron fertilization experiment
759 EisenEx in the Southern Ocean. Deep-Sea Research Part I: Oceanographic Research
760 Papers 54, 340-362.

761 Assmy, P., Smetacek, V., Montresor, M., Klaas, C., Henjes, J., Strass, V.H., Arrieta, J.M.,
762 Bathmann, U., Berg, G.M., Breitbarth, E., Cisewski, B., Friedrichs, L., Fuchs, N., Herndl,

763 G.J., Jansen, S., Krägefsky, S., Latasa, M., Peeken, I., Röttgers, R., Scharek, R., Schüller,
764 S.E., Steigenberger, S., Webb, A., Wolf-Gladrow, D., 2013. Thick-shelled, grazer-
765 protected diatoms decouple ocean carbon and silicon cycles in the iron-limited Antarctic
766 Circumpolar Current. Proceedings of the National Academy of Sciences 110, 20633-
767 20638.

768 Bathmann, U.V., Scharek, R., Klaas, C., Dubischar, C.D., Smetacek, V., 1997. Spring
769 development of phytoplankton biomass and composition in major water masses of the
770 Atlantic sector of the Southern Ocean. Deep-Sea Research Part II: Topical Studies in
771 Oceanography 44, 51-67.

772 Belcher, A., Manno, C., Ward, P., Henson, S., Sanders, R., Tarling, G., 2016.
773 Zooplankton faecal pellet transfer through the meso- and bathypelagic layers in the
774 Southern Ocean in spring. Biogeosciences Discuss. 2016, 1-27.

775 Belcher, A., Tarling, G.A., Manno, C., Atkinson, A., Ward, P., Skaret, G., Fielding, S.,
776 Henson, S.A., Sanders, R., 2017. The potential role of Antarctic krill faecal pellets in
777 efficient carbon export at the marginal ice zone of the South Orkney Islands in spring.
778 Polar Biol, 1-13.

779 Bostock, H.C., Barrows, T.T., Carter, L., Chase, Z., Cortese, G., Dunbar, G.B., Ellwood,
780 M., Hayward, B., Howard, W., Neil, H.L., Noble, T.L., Mackintosh, A., Moss, P.T., Moy,
781 A.D., White, D., Williams, M.J.M., Armand, L.K., 2013. A review of the Australian–
782 New Zealand sector of the Southern Ocean over the last 30 ka (Aus-INTIMATE project).
783 Quaternary Science Reviews 74, 35-57.

784 Boyd, P., Watson, A., Law, C., Abraham, E., Trull, T., Murdoch, R., Bakker, D., Bowie,
785 A., Buesseler, K., Chang, H., 2000. Phytoplankton bloom upon mesoscale iron
786 fertilisation of polar Southern Ocean waters. Nature 407, 695-702.

787 Boyd, P.W., 2013. Diatom traits regulate Southern Ocean silica leakage. Proceedings of
788 the National Academy of Sciences 110, 20358-20359.

789 Boyd, P.W., Law, C.S., 2001. The Southern Ocean Iron RElease Experiment
790 (SOIREE)—introduction and summary. Deep-Sea Research Part II: Topical Studies in
791 Oceanography 48, 2425-2438.

792 Boyd, P.W., Law, C.S., Wong, C., Nojiri, Y., Tsuda, A., Levasseur, M., Takeda, S.,
793 Rivkin, R., Harrison, P.J., Strzepek, R., 2004. The decline and fate of an iron-induced
794 subarctic phytoplankton bloom. Nature 428, 549-553.

795 Boyd, P.W., Newton, P.P., 1999. Does planktonic community structure determine
796 downward particulate organic carbon flux in different oceanic provinces? Deep-Sea
797 Research Part I: Oceanographic Research Papers 46, 63-91.

798 Burckle, L.H., Cirilli, J., 1987. Origin of Diatom Ooze Belt in the Southern Ocean:
799 Implications for Late Quaternary Paleoceanography. Micropaleontology 33, 82-86.

800 Cefarelli, A.O., Ferrario, M.E., Almandoz, G.O., Atencio, A.G., Akselman, R., Vernet,
801 M., 2010. Diversity of the diatom genus *Fragilariopsis* in the Argentine Sea and Antarctic
802 waters: morphology, distribution and abundance. Polar Biol 33, 1463-1484.

803 Coale, K.H., Johnson, K.S., Chavez, F.P., Buesseler, K.O., Barber, R.T., Brzezinski,
804 M.A., Cochlan, W.P., Millero, F.J., Falkowski, P.G., Bauer, J.E., Wanninkhof, R.H.,
805 Kudela, R.M., Altabet, M.A., Hales, B.E., Takahashi, T., Landry, M.R., Bidigare, R.R.,
806 Wang, X., Chase, Z., Strutton, P.G., Friederich, G.E., Gorbunov, M.Y., Lance, V.P.,
807 Hilting, A.K., Hiscock, M.R., Demarest, M., Hiscock, W.T., Sullivan, K.F., Tanner, S.J.,
808 Gordon, R.M., Hunter, C.N., Elrod, V.A., Fitzwater, S.E., Jones, J.L., Tozzi, S., Koblizek,
809 M., Roberts, A.E., Herndon, J., Brewster, J., Ladizinsky, N., Smith, G., Cooper, D.,
810 Timothy, D., Brown, S.L., Selph, K.E., Sheridan, C.C., Twining, B.S., Johnson, Z.I.,
811 2004. Southern Ocean Iron Enrichment Experiment: Carbon Cycling in High- and Low-
812 Si Waters. Science 304, 408-414.

813 Crosta, X., Romero, O., Armand, L.K., Pichon, J.-J., 2005. The biogeography of major
814 diatom taxa in Southern Ocean sediments: 2. Open ocean related species.
815 Palaeogeography, Palaeoclimatology, Palaeoecology 223, 66-92.

816 Chaigneau, A., Morrow, R.A., Rintoul, S.R., 2004. Seasonal and interannual evolution of
817 the mixed layer in the Antarctic Zone south of Tasmania. Deep-Sea Research Part I:
818 Oceanographic Research Papers 51, 2047-2072.

819 Davison, P.C., Checkley, D.M., Koslow, J.A., Barlow, J., 2013. Carbon export mediated
820 by mesopelagic fishes in the northeast Pacific Ocean. Progress in Oceanography 116, 14-
821 30.

DiTullio, G.R., Smith, W.O., 1996. Spatial patterns in phytoplankton biomass and pigment distributions in the Ross Sea. Journal of Geophysical Research: Oceans 101, 18467-18477.

Dugdale, R., Wilkerson, F., 2001. Sources and fates of silicon in the ocean: The role of diatoms in the climate and glacial cycles. Scientia Marina 65, 141-152.

Durkin, C.A., Marchetti, A., Bender, S.J., Truong, T., Morales, R., Mock, T., Armbrust, E.V., 2012. Frustule-related gene transcription and the influence of diatom community composition on silica precipitation in an iron-limited environment. Limnology and Oceanography 57, 1619-1633.

Ebersbach, F., Trull, T.W., Davies, D.M., Bray, S.G., 2011. Controls on mesopelagic particle fluxes in the Sub-Antarctic and Polar Frontal Zones in the Southern Ocean south of Australia in summer—Perspectives from free-drifting sediment traps. Deep-Sea Research Part II: Topical Studies in Oceanography 58, 2260-2276.

Edwards, B.R., Bidle, K.D., Van Mooy, B.A.S., 2015. Dose-dependent regulation of microbial activity on sinking particles by polyunsaturated aldehydes: Implications for the carbon cycle. Proceedings of the National Academy of Sciences.

Fischer, G., Gersonde, R., Wefer, G., 2002. Organic carbon, biogenic silica and diatom fluxes in the marginal winter sea-ice zone and in the Polar Front Region: interannual variations and differences in composition. Deep-Sea Research Part II: Topical Studies in Oceanography 49, 1721-1745.

Flores, J.A., Sierro, F.J., 1997. A revised technique for the calculation of calcareous nannofossil accumulation rates. Micropaleontology 43, 321-324.

Gersonde, R., Zielinski, U., 2000. The reconstruction of late Quaternary Antarctic sea-ice distribution—the use of diatoms as a proxy for sea-ice. Palaeogeography, Palaeoclimatology, Palaeoecology 162, 263-286.

Grigorov, I., Rigual-Hernandez, A.S., Honjo, S., Kemp, A.E.S., Armand, L.K., 2014. Settling fluxes of diatoms to the interior of the Antarctic circumpolar current along 170°W. Deep-Sea Research Part I: Oceanographic Research Papers 93, 1-13.

Hamm, C.E., Merkel, R., Springer, O., Jurkojc, P., Maier, C., Prechtel, K., Smetacek, V., 2003. Architecture and material properties of diatom shells provide effective mechanical protection. Nature 421, 841-843.

Hasle, G.R., Syvertsen, E.E., 1997. Marine diatoms. Identifying marine phytoplankton. Academic Press, San Diego, CA, 5–385.

Hirata, T., Hardman-Mountford, N., Brewin, R., Aiken, J., Barlow, R., Suzuki, K., Isada, T., Howell, E., Hashioka, T., Noguchi-Aita, M., 2011. Synoptic relationships between surface Chlorophyll-a and diagnostic pigments specific to phytoplankton functional types. Biogeosciences 8, 311.

Honjo, S., Doherty, K.W., 1988. Large aperture time-series sediment traps; design objectives, construction and application. Deep-Sea Research Part A. Oceanographic Research Papers 35, 133-149.

Honjo, S., Francois, R., Manganini, S., Dymond, J., Collier, R., 2000. Particle fluxes to the interior of the Southern Ocean in the Western Pacific sector along 170°W. Deep-Sea Research Part II: Topical Studies in Oceanography 47, 3521-3548.

Honjo, S., Manganini, S.J., Krishfield, R.A., Francois, R., 2008. Particulate organic carbon fluxes to the ocean interior and factors controlling the biological pump: A synthesis of global sediment trap programs since 1983. Progress in Oceanography 76, 217-285.

Jackson, G.A., Burd, A.B., 2001. A model for the distribution of particle flux in the mid-water column controlled by subsurface biotic interactions. Deep-Sea Research Part II: Topical Studies in Oceanography 49, 193-217.

Jordan, R., Stickley, C., 2010. Diatoms as indicators of paleoceanographic events. The Diatoms: Applications for the Environmental and Earth Sciences. Cambridge University Press, Cambridge.

Kang, S.-H., Fryxell, G.A., 1992. Fragilariopsis cylindrus (Grunow) Krieger: The most abundant diatom in water column assemblages of Antarctic marginal ice-edge zones. Polar Biol 12, 609-627.

878 Kang, S.-H., Kang, J.-S., Lee, S., Chung, K.H., Kim, D., Park, M.G., 2001. Antarctic
879 Phytoplankton Assemblages in the Marginal Ice Zone of the Northwestern Weddell Sea.
880 Journal of Plankton Research 23, 333-352.

881 Kang, S.H., Lee, S.H., 1995. Antarctic phytoplankton assemblage in the western
882 Bransfield Strait region, February 1993: composition, biomass, and mesoscale
883 distributions. Marine Ecology Progress Series 129, 253-267.

884 Kopczynska, E.E., Dehairs, F., Elskens, M., Wright, S., 2001. Phytoplankton and
885 microzooplankton variability between the Subtropical and Polar Fronts south of
886 Australia: Thriving under regenerative and new production in late summer. Journal of
887 Geophysical Research: Oceans 106, 31597-31609.

888 Kopczyńska, E.E., Savoye, N., Dehairs, F., Cardinal, D., Elskens, M., 2007. Spring
889 phytoplankton assemblages in the Southern Ocean between Australia and Antarctica.
890 Polar Biol 31, 77-88.

891 Kropuenske, L.R., Mills, M.M., van Dijken, G.L., Alderkamp, A.-C., Mine Berg, G.,
892 Robinson, D.H., Welschmeyer, N.A., Arrigo, K.R., 2010. Strategies and rates of
893 photoacclimation in two major Southern Ocean phytoplankton taxa: Phaeocystis
894 antarctica (Haptophyta) and Fragilariopsis cylindrus (bacillariophyceae)1. Journal of
895 Phycology 46, 1138-1151.

896 Lampitt, R.S., Salter, I., Johns, D., 2009. Radiolaria: Major exporters of organic carbon
897 to the deep ocean. Global Biogeochemical Cycles 23, GB1010.

898 Landry, M.R., Selph, K.E., Brown, S.L., Abbott, M.R., Measures, C.I., Vink, S., Allen,
899 C.B., Calbet, A., Christensen, S., Nolla, H., 2002. Seasonal dynamics of phytoplankton
900 in the Antarctic Polar Front region at 170°W. Deep-Sea Research Part II: Topical Studies
901 in Oceanography 49, 1843-1865.

902 Laurenceau-Cornec, E.C., Trull, T., Davies, D.M., Bray, S.G., Doran, J., Planchon, F.,
903 Carlotti, F., Jouander, M., Cavagna, A.-J., Waite, A., 2015. The relative importance of
904 phytoplankton aggregates and zooplankton fecal pellets to carbon export: insights from
905 free-drifting sediment trap deployments in naturally iron-fertilised waters near the
906 Kerguelen Plateau. Biogeosciences 12, 1007-1027.

907 Leventer, A., 1998. The fate of Antarctic “sea ice diatoms” and their use as
908 paleoenvironmental indicators. Antarctic sea ice: biological processes, interactions and
909 variability, 121-137.

910 Loscher, B.M., De Baar, H.J.W., De Jong, J.T.M., Veth, C., Dehairs, F., 1997. The
911 distribution of Fe in the Antarctic circumpolar current. Deep-Sea Research Part II:
912 Topical Studies in Oceanography 44, 143-187.

913 Lowry, K.E., Pickart, R.S., Selz, V., Mills, M.M., Pacini, A., Lewis, K.M., Joy-Warren,
914 H.L., Nobre, C., Dijken, G.L.v., Grondin, P.L., Ferland, J., Arrigo, K.R., 2018. Under-Ice
915 Phytoplankton Blooms Inhibited by Spring Convective Mixing in Refreezing Leads.
916 Journal of Geophysical Research: Oceans 123, 90-109.

917 Mangoni, O., Saggiomo, M., Modigh, M., Catalano, G., Zingone, A., Saggiomo, V.,
918 2009. The role of platelet ice microalgae in seeding phytoplankton blooms in Terra Nova
919 Bay (Ross Sea, Antarctica): a mesocosm experiment. Polar Biol 32, 311-323.

920 Manno, C., Stowasser, G., Enderlein, P., Fielding, S., Tarling, G.A., 2015. The
921 contribution of zooplankton faecal pellets to deep-carbon transport in the Scotia Sea
922 (Southern Ocean). Biogeosciences 12, 1955-1965.

923 McLeod, D.J., Hosie, G.W., Kitchener, J.A., Takahashi, K.T., Hunt, B.P.V., 2010.
924 Zooplankton Atlas of the Southern Ocean: The SCAR SO-CPR Survey (1991–2008).
925 Polar Science 4, 353-385.

926 McMinn, A., 1995. Comparison of diatom preservation between oxic and anoxic basins
927 in Ellis Fjord, Antarctica. Diatom Research 10, 145-151.

928 Mills, M.M., Kropuenske, L.R., van Dijken, G.L., Alderkamp, A.-C., Berg, G.M.,
929 Robinson, D.H., Welschmeyer, N.A., Arrigo, K.R., 2010. Photophysiology in two
930 Southern Ocean phytoplankton taxa: Photosynthesis of Phaeocystis antarctica
931 (prymnesiophyceae) and Fragilariopsis cylindrus (Bacillariophyceae) under simulated
932 mixed-layer irradiance1. Journal of Phycology 46, 1114-1127.

933 Mohan, R., Shanvas, S., Thamban, M., Sudhakar, M., 2006. Spatial distribution of
934 diatoms in surface sediments from the Indian sector of Southern Ocean. Current Science
935 91, 1495-1502.

936 Moore, T.C., 1973. Method of randomly distributing grains for microscopic examination.
937 Journal of Sedimentary Research 43.

938 Nelson, D.M., Anderson, R.F., Barber, R.T., Brzezinski, M.A., Buesseler, K.O., Chase,
939 Z., Collier, R.W., Dickson, M.-L., François, R., Hiscock, M.R., Honjo, S., Marra, J.,
940 Martin, W.R., Sambrotto, R.N., Sayles, F.L., Sigmon, D.E., 2002. Vertical budgets for
941 organic carbon and biogenic silica in the Pacific sector of the Southern Ocean, 1996–
942 1998. Deep-Sea Research Part II: Topical Studies in Oceanography 49, 1645-1674.

943 Nomura, D., Aoki, S., Simizu, D., Iida, T., 2018. Influence of Sea Ice Crack Formation
944 on the Spatial Distribution of Nutrients and Microalgae in Flooded Antarctic Multiyear
945 Ice. Journal of Geophysical Research: Oceans 123, 939-951.

946 Nowlin, W.D.J., Clifford, M., 1982. The kinematic and thermohaline zonation of the
947 Antarctic Circumpolar Current at Drake Passage. Journal of Marine Research 40, 481-
948 507.

949 Orsi, A.H., Whitworth Iii, T., Nowlin Jr, W.D., 1995. On the meridional extent and fronts
950 of the Antarctic Circumpolar Current. Deep-Sea Research Part I: Oceanographic
951 Research Papers 42, 641-673.

952 Parslow, J.S., Boyd, P.W., Rintoul, S.R., Griffiths, F.B., 2001. A persistent subsurface
953 chlorophyll maximum in the Interpolar Frontal Zone south of Australia: Seasonal
954 progression and implications for phytoplankton-light-nutrient interactions. Journal of
955 Geophysical Research: Oceans 106, 31543-31557.

956 Passow, U., Engel, A., Ploug, H., 2003. The role of aggregation for the dissolution of
957 diatom frustules. FEMS Microbiology Ecology 46, 247-255.

958 Pike, J., Allen, C.S., Leventer, A., Stickley, C.E., Pudsey, C.J., 2008. Comparison of
959 contemporary and fossil diatom assemblages from the western Antarctic Peninsula shelf.
960 Marine Micropaleontology 67, 274-287.

961 Pilskaln, C.H., Manganini, S.J., Trull, T.W., Armand, L., Howard, W., Asper, V.L.,
962 Massom, R., 2004. Geochemical particle fluxes in the Southern Indian Ocean seasonal
963 ice zone: Prydz Bay region, East Antarctica. Deep-Sea Research Part I: Oceanographic
964 Research Papers 51, 307-332.

965 Pollard, R., Tréguer, P., Read, J., 2006. Quantifying nutrient supply to the Southern
966 Ocean. Journal of Geophysical Research: Oceans 111, C05011.

967 Pollard, R.T., Bathmann, U., Dubischar, C., Read, J.F., Lucas, M., 2002. Zooplankton
968 distribution and behaviour in the Southern Ocean from surveys with a towed Optical
969 Plankton Counter. Deep-Sea Research Part II: Topical Studies in Oceanography 49, 3889-
970 3915.

971 Popp, B.N., Trull, T., Kenig, F., Wakeham, S.G., Rust, T.M., Tilbrook, B., Griffiths, B.,
972 Wright, S.W., Marchant, H.J., Bidigare, R.R., Laws, E.A., 1999. Controls on the carbon
973 isotopic composition of southern ocean phytoplankton. Global Biogeochemical Cycles
974 13, 827-843.

975 Quéguiner, B., 2013. Iron fertilization and the structure of planktonic communities in
976 high nutrient regions of the Southern Ocean. Deep-Sea Research Part II: Topical Studies
977 in Oceanography 90, 43-54.

978 Ragueneau, O., Dittert, N., Pondaven, P., Tréguer, P., Corrin, L., 2002. Si/C decoupling
979 in the world ocean: is the Southern Ocean different? Deep-Sea Research Part II: Topical
980 Studies in Oceanography 49, 3127-3154.

981 Rembauville, M., Blain, S., Armand, L., Quéguiner, B., Salter, I., 2014. Export fluxes in
982 a naturally fertilized area of the Southern Ocean, the Kerguelen Plateau: ecological
983 vectors of carbon and biogenic silica to depth (Part 2). Biogeosciences Discuss. 11,
984 17089-17150.

985 Rembauville, M., Manno, C., Tarling, G.A., Blain, S., Salter, I., 2016. Strong contribution
986 of diatom resting spores to deep-sea carbon transfer in naturally iron-fertilized waters
987 downstream of South Georgia. Deep-Sea Research Part I: Oceanographic Research
988 Papers 115, 22-35.

989 Riaux-Gobin, C., Poulin, M., Dieckmann, G., Labrune, C., Vétion, G., 2011. Spring
990 phytoplankton onset after the ice break-up and sea-ice signature (Adélie Land, East
991 Antarctica). 2011.

992 Rigual-Hernández, A.S., Trull, T.W., Bray, S.G., Armand, L.K., 2016. The fate of diatom
993 valves in the Subantarctic and Polar Frontal Zones of the Southern Ocean: Sediment trap
994 versus surface sediment assemblages. Palaeogeography, Palaeoclimatology,
995 Palaeoecology 457, 129-143.

996 Rigual-Hernández, A.S., Trull, T.W., Bray, S.G., Closset, I., Armand, L.K., 2015a.
997 Seasonal dynamics in diatom and particulate export fluxes to the Deep-Sea in the
998 Australian sector of the southern Antarctic Zone. Journal of Marine Systems 142, 62-74.

999 Rigual-Hernández, A.S., Trull, T.W., Bray, S.G., Cortina, A., Armand, L.K., 2015b.
1000 Latitudinal and temporal distributions of diatom populations in the pelagic waters of the
1001 Subantarctic and Polar Frontal Zones of the Southern Ocean and their role in the
1002 biological pump. Biogeosciences 12, 8615-8690.

1003 Romero, O., 1998. Marine Planktonic Diatoms from the Tropical and Equatorial Atlantic:
1004 Temporal Flux Patterns and the Sediment Record. . University of Bremen Press, p. 203.

1005 Rousseaux, C.S., Gregg, W.W., 2012. Climate variability and phytoplankton composition
1006 in the Pacific Ocean. Journal of Geophysical Research: Oceans 117, C10006.

1007 Salter, I., Kemp, A.E.S., Moore, C.M., Lampitt, R.S., Wolff, G.A., Holtvoeth, J., 2012.
1008 Diatom resting spore ecology drives enhanced carbon export from a naturally iron-
1009 fertilized bloom in the Southern Ocean. Global Biogeochemical Cycles 26, GB1014.

1010 Salter, I., Schiebel, R., Ziveri, P., Movellan, A., Lampitt, R., Wolff, G.A., 2014.
1011 Carbonate counter pump stimulated by natural iron fertilization in the Polar Frontal Zone.
1012 Nature Geosci 7, 885-889.

1013 Sancetta, C., Calvert, S.E., 1988. The annual cycle of sedimentation in Saanich inlet,
1014 British Columbia: implications for the interpretation of diatom fossil assemblages. Deep-
1015 Sea Research Part A. Oceanographic Research Papers 35, 71-90.

1016 Sarmiento, J.L., Gruber, N., Brzezinski, M.A., Dunne, J.P., 2004. High-latitude controls
1017 of thermocline nutrients and low latitude biological productivity. Nature 427, 56-60.

1018 Scott, P., McMinn, A., Hosie, G., 1994. Physical parameters influencing diatom
1019 community structure in eastern Antarctic sea ice. Polar Biol 14, 507-517.

1020 Schrader, H.J., Gersonde, R., 1978. Diatoms and silicoflagellates. Utrecht
1021 Micropaleontological Bulletins.

1022 Sedwick, P.N., DiTullio, G.R., 1997. Regulation of algal blooms in Antarctic Shelf
1023 Waters by the release of iron from melting sea ice. Geophysical Research Letters 24,
1024 2515-2518.

1025 Selph, K.E., Landry, M.R., Allen, C.B., Calbet, A., Christensen, S., Bidigare, R.R., 2001.
1026 Microbial community composition and growth dynamics in the Antarctic Polar Front and
1027 seasonal ice zone during late spring 1997. Deep-Sea Research Part II: Topical Studies in
1028 Oceanography 48, 4059-4080.

1029 Siegel, D.A., Buesseler, K.O., Doney, S.C., Sailley, S.F., Behrenfeld, M.J., Boyd, P.W.,
1030 2014. Global assessment of ocean carbon export by combining satellite observations and
1031 food-web models. Global Biogeochemical Cycles 28, 181-196.

1032 Smetacek, V., Klaas, C., Menden-Deuer, S., Rynearson, T.A., 2002. Mesoscale
1033 distribution of dominant diatom species relative to the hydrographical field along the
1034 Antarctic Polar Front. Deep-Sea Research Part II: Topical Studies in Oceanography 49,
1035 3835-3848.

1036 Smetacek, V., Klaas, C., Strass, V.H., Assmy, P., Montresor, M., Cisewski, B., Savoye,
1037 N., Webb, A., d/'Ovidio, F., Arrieta, J.M., Bathmann, U., Bellerby, R., Berg, G.M., Croot,
1038 P., Gonzalez, S., Henjes, J., Herndl, G.J., Hoffmann, L.J., Leach, H., Losch, M., Mills,
1039 M.M., Neill, C., Peeken, I., Rottgers, R., Sachs, O., Sauter, E., Schmidt, M.M., Schwarz,
1040 J., Terbruggen, A., Wolf-Gladrow, D., 2012. Deep carbon export from a Southern Ocean
1041 iron-fertilized diatom bloom. Nature 487, 313-319.

1042 Smith Jr, W.O., Anderson, R.F., Keith Moore, J., Codispoti, L.A., Morrison, J.M., 2000.
1043 The US Southern Ocean Joint Global Ocean Flux Study: an introduction to AESOPS.
1044 Deep-Sea Research Part II: Topical Studies in Oceanography 47, 3073-3093.

1045 Speer, K., Rintoul, S.R., Sloyan, B., 2000. The Diabatic Deacon Cell. Journal of Physical
1046 Oceanography 30, 3212-3222.

1047 Takahashi, K., Fujitani, N., Yanada, M., Maita, Y., 2000. Long-term biogenic particle
1048 fluxes in the Bering Sea and the central subarctic Pacific Ocean, 1990-1995. Deep-Sea
1049 Research Part I: Oceanographic Research Papers 47, 1723-1759.

1050 Takahashi, T., Sutherland, S.C., Sweeney, C., Poisson, A., Metzl, N., Tilbrook, B., Bates,
1051 N., Wanninkhof, R., Feely, R.A., Sabine, C., Olafsson, J., Nojiri, Y., 2002. Global sea–
1052 air CO2 flux based on climatological surface ocean pCO2, and seasonal biological and
1053 temperature effects. Deep-Sea Research Part II: Topical Studies in Oceanography 49,
1054 1601-1622.

1055 Taylor, F., McMinn, A., Franklin, D., 1997. Distribution of diatoms in surface sediments
1056 of Prydz Bay, Antarctica. Marine Micropaleontology 32, 209-229.

1057 Tréguer, P.J., 2014. The Southern Ocean silica cycle. Comptes Rendus Geoscience 346,
1058 279-286.

1059 Trull, T.W., Rintoul, S.R., Hadfield, M., Abraham, E.R., 2001. Circulation and seasonal
1060 evolution of polar waters south of Australia: implications for iron fertilization of the
1061 Southern Ocean. Deep-Sea Research Part II: Topical Studies in Oceanography 48, 2439-
1062 2466.

1063 Ugalde, S.C., Westwood, K.J., van den Enden, R., McMinn, A., Meiners, K.M., 2016.
1064 Characteristics and primary productivity of East Antarctic pack ice during the winter-
1065 spring transition. Deep-Sea Research Part II: Topical Studies in Oceanography 131, 123-
1066 139.

1067 van der Merwe, P., Lannuzel, D., Bowie, A.R., Meiners, K.M., 2011. High temporal
1068 resolution observations of spring fast ice melt and seawater iron enrichment in East
1069 Antarctica. Journal of Geophysical Research: Biogeosciences 116, n/a-n/a.

1070 Villafañe, V.E., Helbling, E.W., Holm-Hansen, O., 1995. Spatial and temporal variability
1071 of phytoplankton biomass and taxonomic composition around Elephant Island,
1072 Antarctica, during the summers of 1990–1993. Marine Biology 123, 677-686.

1073 Wassmann, P., 1998. Retention versus export food chains: processes controlling sinking
1074 loss from marine pelagic systems, in: Tamminen, T., Kuosa, H. (Eds.), Eutrophication in
1075 Planktonic Ecosystems: Food Web Dynamics and Elemental Cycling: Proceedings of the
1076 Fourth International PELAG Symposium, held in Helsinki, Finland, 26–30 August 1996.
1077 Springer Netherlands, Dordrecht, pp. 29-57.

1078 Wilson, D.L., Smith, W.O., Nelson, D.M., 1986. Phytoplankton bloom dynamics of the
1079 western Ross Sea ice edge—I. Primary productivity and species-specific production.
1080 Deep-Sea Research Part A. Oceanographic Research Papers 33, 1375-1387.

1081 Zielinski, U., Gersonde, R., 1997. Diatom distribution in Southern Ocean surface
1082 sediments (Atlantic sector): Implications for paleoenvironmental reconstructions.
1083 Palaeogeography, Palaeoclimatology, Palaeoecology 129, 213-250.

1084

1085

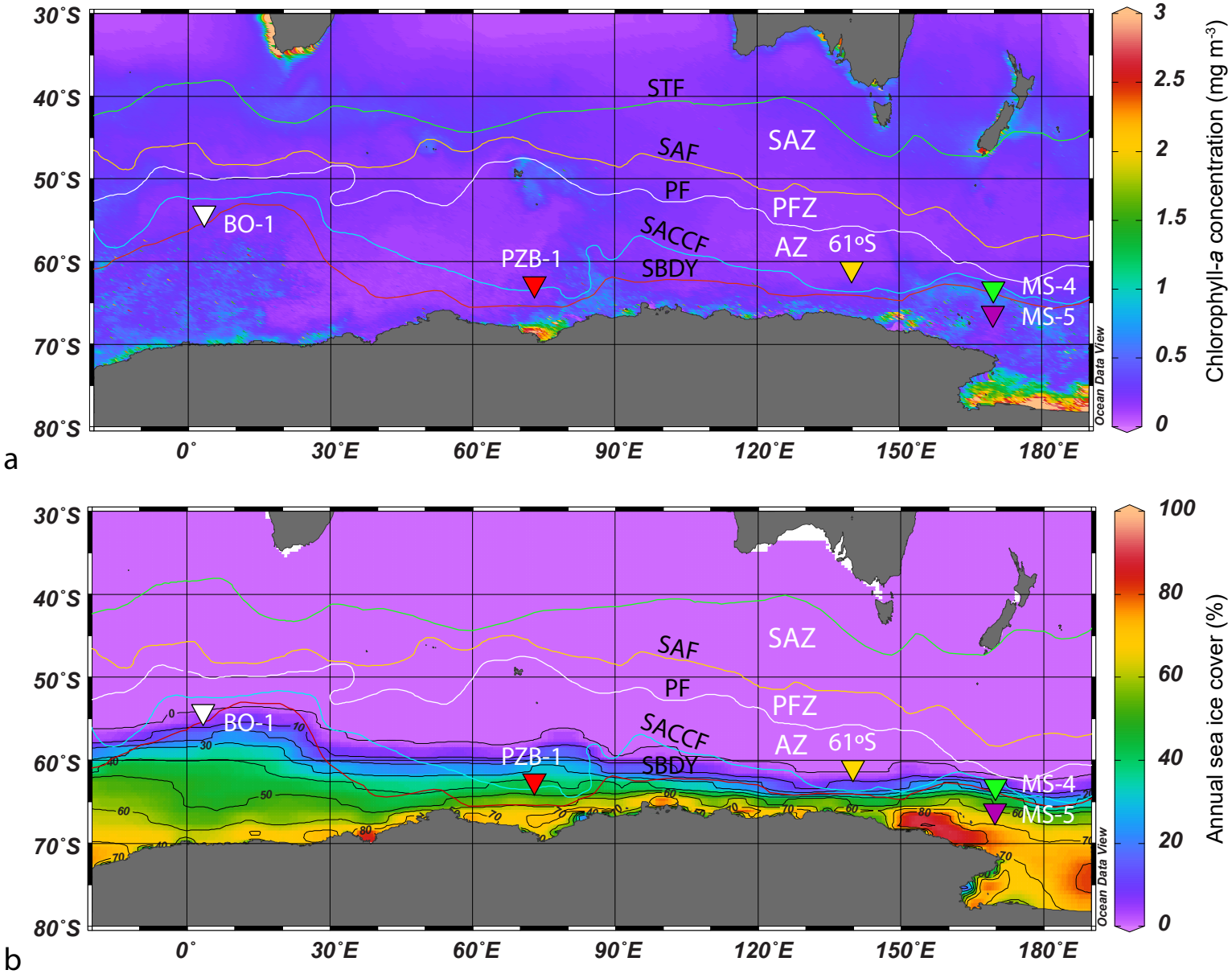
30˚S
40˚S
50˚S
60˚S
70˚S
80˚S
0˚
30˚E
60˚E
90˚E
120˚E
150˚E
180˚E
STF
SAF
PF
SACCF
SBDY
SAZ
PFZ
AZ
61ºS
BO-1
PZB-1
MS-4
MS-5
Ocean Data View
3
2.5
2
1.5
1
0.5
0
Chlorophyll-a concentration (mg m-3)
a
100
80
60
40
20
0
Annual sea ice cover (%)
b

Figure 1

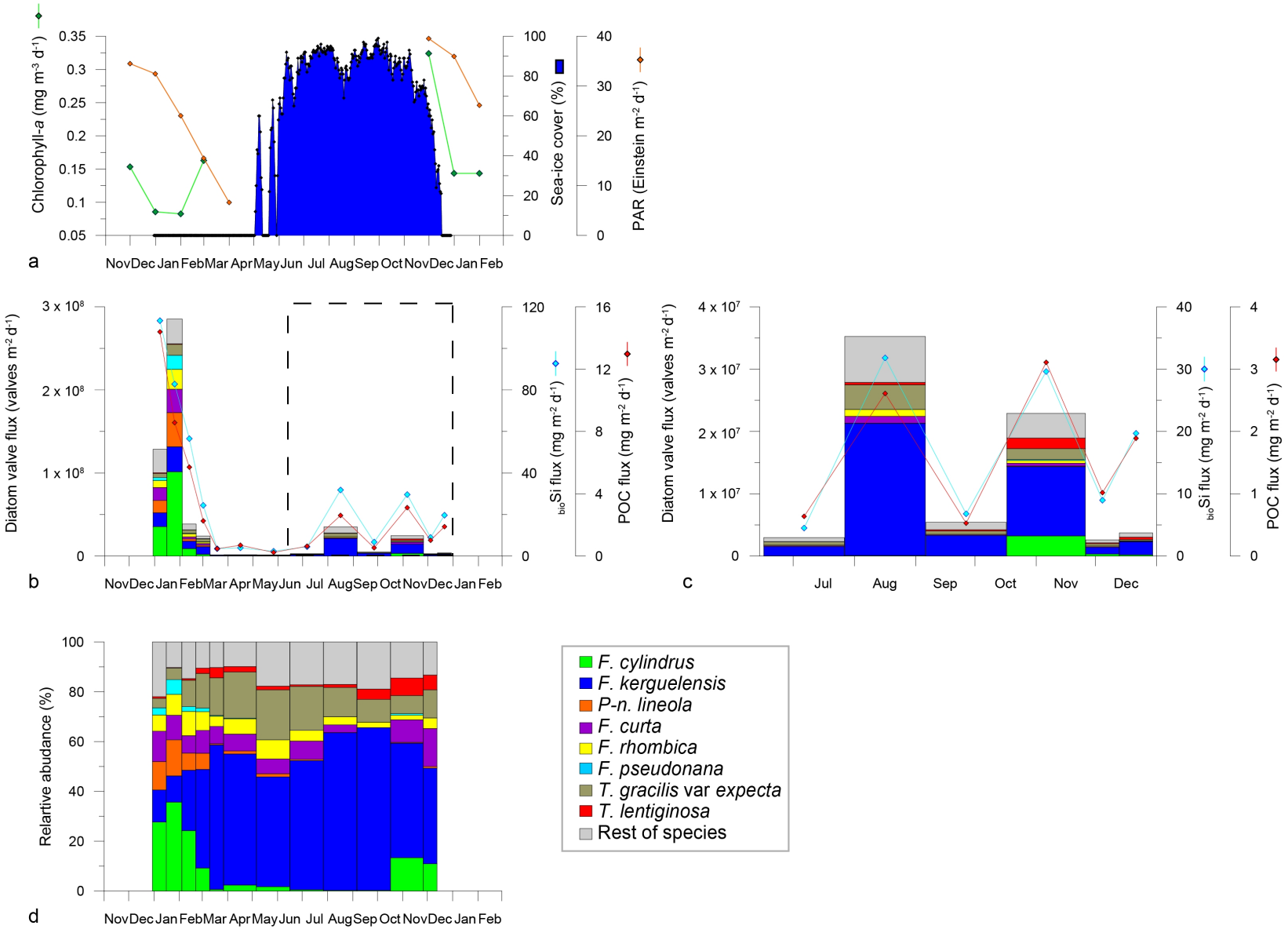
a
Chlorophyll-a (mg m-3 d-1)
Sea-ice cover (%)
PAR (Einstein m-2 d-1)
Nov Dec Jan Feb Mar Apr May Jun Jul Aug Sep Oct Nov Dec Jan Feb
b
Diatom valve flux (valves m-2 d-1)
bioSi flux (mg m-2 d-1)
POC flux (mg m-2 d-1)
c
Jul Aug Sep Oct Nov Dec
d
Relartive abudance (%)
F. cylindrus
F. kerguelensis
P-n. lineola
F. curta
F. rhombica
F. pseudonana
T. gracilis var expecta
T. lentiginosa
Rest of species

Figure 2

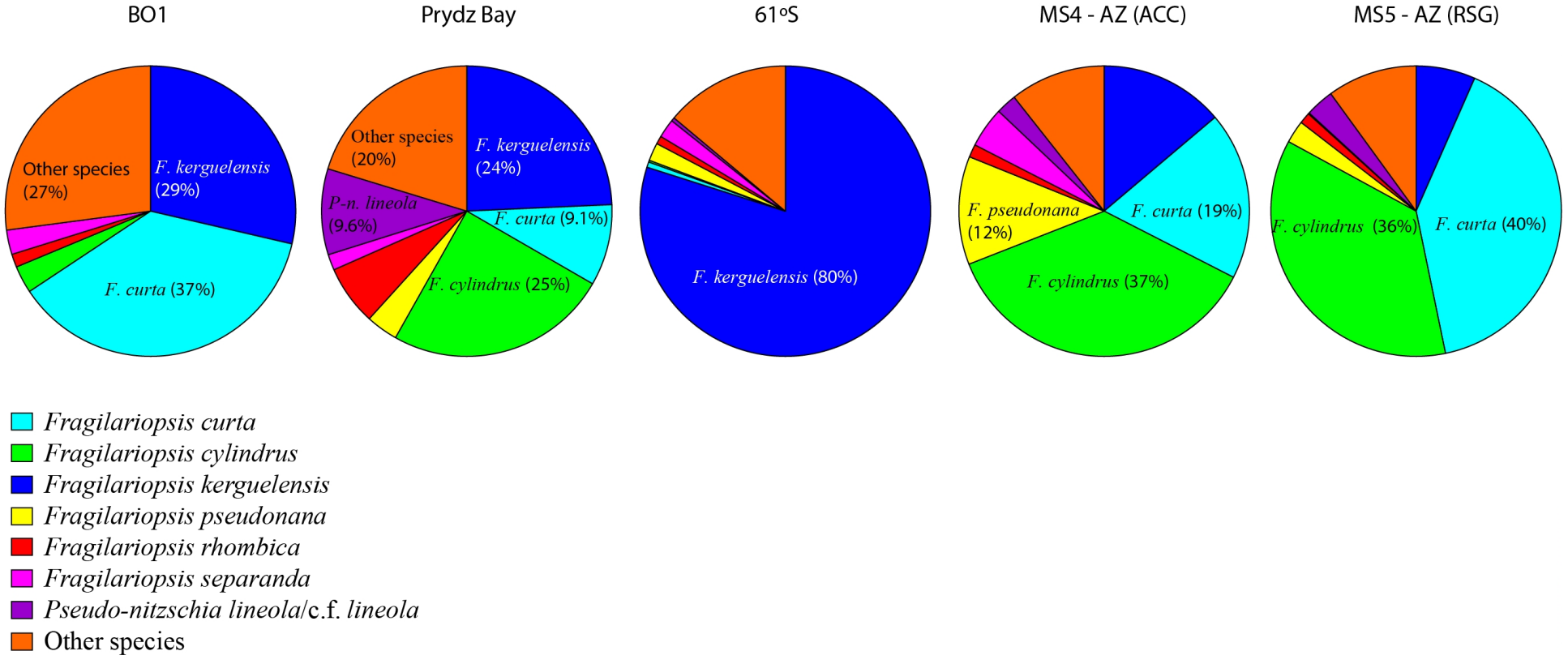
BO1
Prydz Bay
61°S
MS4 - AZ (ACC)
MS5 - AZ (RSG)
Other species (27%)
F. kerguelensis (29%)
F. curta (37%)
Other species (20%)
F. kerguelensis (24%)
P-n. lineola (9.6%)
F. curta (9.1%)
F. cylindrus (25%)
F. kerguelensis (80%)
F. pseudonana (12%)
F. curta (19%)
F. cylindrus (37%)
F. cylindrus (36%)
F. curta (40%)
Fragilariopsis curta
Fragilariopsis cylindrus
Fragilariopsis kerguelensis
Fragilariopsis pseudonana
Fragilariopsis rhombica
Fragilariopsis separanda
Pseudo-nitzschia lineola/c.f. lineola
Other species

Figure 3.

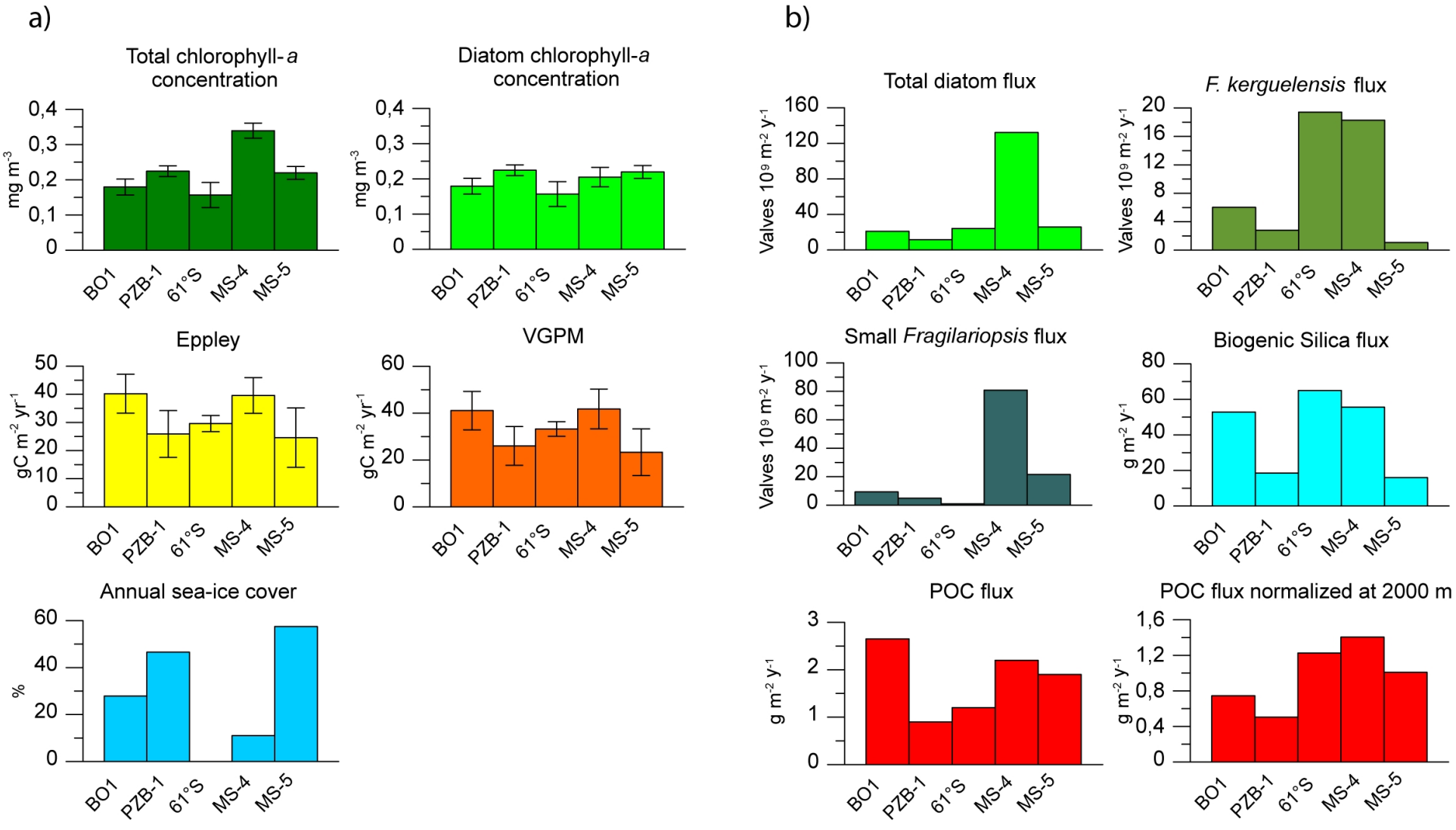
a)
Total chlorophyll-a concentration
mg m-3
0,4
0,3
0,2
0,1
0
BO1
PZB-1
61°S
MS-4
MS-5
Diatom chlorophyll-a concentration
mg m-3
0,4
0,3
0,2
0,1
0
BO1
PZB-1
61°S
MS-4
MS-5
Eppley
gC m-2 yr-1
50
40
30
20
10
0
BO1
PZB-1
61°S
MS-4
MS-5
VGPM
gC m-2 yr-1
60
40
20
0
BO1
PZB-1
61°S
MS-4
MS-5
Annual sea-ice cover
%
60
40
20
0
BO1
PZB-1
61°S
MS-4
MS-5
b)
Total diatom flux
Valves 10⁹ m-2 y-1
160
120
80
40
0
BO1
PZB-1
61°S
MS-4
MS-5
F. kerguelensis flux
Valves 10⁹ m-2 y-1
20
16
12
8
4
0
BO1
PZB-1
61°S
MS-4
MS-5
Small Fragilariopsis flux
Valves 10⁹ m-2 y-1
100
80
60
40
20
0
BO1
PZB-1
61°S
MS-4
MS-5
Biogenic Silica flux
g m-2 y-1
80
60
40
20
0
BO1
PZB-1
61°S
MS-4
MS-5
POC flux
g m-2 y-1
3
2
1
0
BO1
PZB-1
61°S
MS-4
MS-5
POC flux normalized at 2000 m
g m-2 y-1
1,6
1,2
0,8
0,4
0
BO1
PZB-1
61°S
MS-4
MS-5

Station	Latitude	Longitude	Water column depth (m)	Trap depth (m)	Sampling interval start	Sampling interval end
BO-1	54° 20´S	3° 23’E	2734	450	28/12/1990	01/04/1992
PZB-1	62°29’S	72°59’E	4000	1400	30/12/1998	13/12/1999
61°S	60° 44´S	139° 54´E	4393	2000	30/11/2001	29/09/2002
MS-4	63° 09´S	169° 54´W	2885	1031	28/11/1996	24/12/1997
MS-5	66° 10´S	169° 40´W	3015	937	28/11/1996	24/12/1997

References
Fischer et al. (2002)
Pilskaln et al (2004) and this study
Rigual-Hernández et al. (2015)
Honjo et al. (2000) and Grigorov et al. (2014)
Honjo et al. (2000) and Grigorov et al. (2014)

Cup number	Mid-point date	Collection days (days)	Total diatom flux (10^6 x valves m^{-2} d^{-1})	*Fragilariopsis curta* (10^6 x valves m^{-2} d^{-1})	*Fragilariopsis cylindrus* (10^6 x valves m^{-2} d^{-1})	*Fragilariopsis kerguelensis* (10^6 x valves m^{-2} d^{-1})	*Fragilariopsis pseudonana* (10^6 x valves m^{-2} d^{-1})	*Fragilariopsis rhombica* (10^6 x valves m^{-2} d^{-1})	*Pseudo-nitzschia lineola* (10^6 x valves m^{-2} d^{-1})	*Thalassisora gracilis* var. *expecta* (10^6 x valves m^{-2} d^{-1})	*Thalassiosira lentiginosa* (10^6 x valves m^{-2} d^{-1})
1	07/01/1999	17.0	128.6	15.8	35.5	16.6	3.7	8.3	14.6	4.9	0.9
2	25/01/1999	19.0	284.6	28.2	101.6	30.1	16.9	23.8	41.1	12.5	0.6
3	12/02/1999	17.0	37.2	2.6	9.0	9.0	0.7	3.6	2.5	2.5	0.2
4	01/03/1999	17.0	23.4	2.2	2.2	9.3	0.3	1.8	1.5	2.5	0.5
5	18/03/1999	17.0	1.5	0.1	0.0	0.9	0.0	0.1	0.0	0.1	0.1
6	16/04/1999	40.0	1.5	0.1	0.0	0.8	0.0	0.1	0.0	0.2	0.0
7	26/05/1999	41.0	1.4	0.1	0.0	0.6	0.0	0.1	0.0	0.2	0.0
8	06/07/1999	41.0	2.9	0.2	0.0	1.5	0.0	0.1	0.0	0.4	0.0
9	16/08/1999	41.0	33.5	1.0	0.1	21.2	0.0	1.1	0.0	2.3	0.4
10	26/09/1999	41.0	5.1	0.0	0.0	3.3	0.0	0.1	0.0	0.3	0.2
11	06/11/1999	40.0	24.2	2.2	3.2	11.1	0.2	0.4	0.1	1.3	1.7
12	04/12/1999	17.0	2.8	0.4	0.3	1.1	0.0	0.1	0.0	0.2	0.2
13	21/12/1999	17.0	3.9	0.3	0.2	2.1	0.0	0.1	0.0	0.1	0.4

Species	BO1	PZB-1	61°S	MS-4	MS-5
Actinocyclus actinochilus (Ehrenberg) Simonsen		0.12	*	*	*
Actinocyclus curvatulus Janisch		*	o	*	o
Actinocyclus exiguus Fryxell et Semina		o	o	o	o
Actinocyclus octonarius Ehrenberg		o	o	*	o
Actinocyclus spp.		o	*	*	*
Alveus marinus (Grunow) Kaczmarska et Fryxell		o	o	o	o
Asteromphalus hookeri Ehrenberg		0.21	0.2	0.16	1.11
A. hyalinus Karsten		*	0.2	*	o
A. parvulus Karsten		0.34	0.2	*	*
Asteromphalus spp.		o	*	o	o
Azpeitia tabularis (Grunow) Fryxell et Sims	0.33	*	0.7	0.15	*
Banquisia belgicae (Van Heurck) Paddock		0.38	o	o	o
Chaetoceros aequatorialis var. *antarcticus* Manguin		o	*	o	o
C. atlanticus Cleve		0.95	0.2	0.19	*
C. criophilus Castracane		o	o	*	*
C. diadema Ehrenberg		o	o	o	*
C. dichaeta Ehrenberg		*	0.1	o	o
C. peruvianus Brightwell		*	o	o	o
Chaetoceros subgenus *Hyalochaete* spp.		0.49	0.2	*	0.13
Chaetoceros subgenus *Phaeoceros* spp.			0.2		
Chaetoceros resting spores		2.59	0.1	o	o
Cocconeis spp.		o	o	o	o
Corethron sp.		0.25	*	*	*
Coscinodiscus asteromphalus Ehrenberg		*	o	o	o
Cyclotella spp.		o	o	o	o
Dactyliosolen antarcticus Castracane		o	o	o	o
Diploneis bombus (Ehrenberg) Ehrenberg		o	o	o	o
Eucampia antarctica (Castracane) Mangin (summer form)		*	o	*	o
E. antarctica (Castracane) Mangin (winter form)			0.1		o
Fragilariopsis curta (Van Heurck) Hustedt	37.05	9.05	0.6	18.70	35.21
F. cylindrus (Grunow) Krieger	3.04	24.83	0.2	36.52	47.04
F. doliolus (Wallich) Medlin et Sims		o	o	o	o
F. kerguelensis (O'Meara) Hustedt	28.63	24.29	79.9	13.83	4.13
F. obliquecostata (van Heurck) Heiden		*	*	*	0.16
F. pseudonana (Hasle) Hasle		3.55	2	12.05	2.96
F. rhombica (O'Meara) Hustedt	1.47	6.67	0.9	1.43	0.79
F. ritscherii Hustedt		0.94	0.1	0.73	1.33
F. separanda Hustedt	2.72	1.76	2.1	4.53	0.18
Fragilariopsis sublinearis (Van Heurck) Heiden et Kolbe		0.57	o	o	o
F. cf. *sublineata* (Van Heurck) Heiden		o	*	o	o
Fragilariopsis vanheurckii (Peragallo) Hustedt		0.26	o	o	o
Fragilariopsis spp.		o	o	o	o
Guinardia spp.		o	o	o	*
Gyrosigma spp.		o	o	o	o
Haslea trompii (Cleve) Simonsen		0.16	*	o	o
Hemidiscus cuneiformis Wallich		o	o	o	o
Manguinea spp.		*	o	o	o
Membraneis spp.		0.33	o	o	o
Navicula directa (Smith) Ralfs in Pritchard		0.23	0.3	o	o
Navicula spp.		*	o	0.55	0.55
Nitzschia bicapitata Cleve		o	o	o	o
N. braarudii (Hasle)		o	o	o	o
N. kolaczeckii Grunow		o	o	o	o
N. sicula (Castracane) Hustedt var. *bicuneata* Grunow		o	0.1	o	o
N. sicula (Castracane) Hustedt var. *rostrata* Hustedt		0.10	o	o	o
Nitzschia spp.		o	o	o	o
Paralia spp.		0.04	o	o	o
Pleurosigma spp.		o	*	0.01	o
Pleurosigma directum		0.03	o	o	o
Porosira pseudodenticulata (Hustedt) Jousé		o	*	o	o
Proboscia alata (Brightwell) Sundström		*	o	o	o
P. inermis (Castracane) Jordan et Ligowski		*	o	o	o

Species	BO1	PZB-1	61°S	MS-4	MS-5
P. truncata (G.Karsten) Nöthig et Ligowski		*	o	o	o
Proboscia spp.		*	o	o	o
Psammodiction panduriforme (Gregory) Mann		o	o	o	o
Pseudo-nitzschia cf. *lineola*		o	0.4	o	o
P-n. lineola (Cleve) Hasle		9.57	o	2.30	3.18
P-n. turgiduloides (Hasle) Hasle		1.58	o	o	o
P-n. prolongatoides (Hasle) Hasle		0.22	o	o	o
P-n. heimii Manguin		o	*	o	o
Pseudo-nitzschia spp.		*	0.1	o	0.13
Rhizosolenia antennata (Ehrenberg) Brown f. *antennata*		*	o	o	o
R. antennata (Ehrenberg) Brown f. *semispina* Sundström		0.70	o	o	o
R. bergonii Peragallo		o	o	o	o
Rhizosolenia cf. *costata*		o	o	o	o
Rhizosolenia cf. chunii		0.23	o	o	o
R. curvata Zacharias		o	o	o	o
R. polydactyla Castracane f. *polydactyla*		o	o	o	o
R. polydactyla Castracane f. *squamosa*		*	o	o	o
R. simplex Karsten		o	o	*	o
R. sima Castracane		o	o	o	*
R. styliformis Brightwell		o	o	*	o
Rhizosolenia sp. f. 1A *sensu* Armand et Zielinski		*	*	o	o
Rhizosolenia spp.		o	0.1	o	o
Roperia tesselata (Roper) Grunow		o	o	o	o
Stellarima stellaris (Roper) Hasle et Sims		o	o	o	o
Synedropsis sp.		*	o	o	o
Thalassionema nitzschioides var. *capitulata* (Castracane) Moreno-Ruiz		o	0.1	o	o
T. nitzschioides var. *lanceolata* (Grunow) Pergallo et Pergallo		o	0.1	*	o
T. nitzschioides var. *parvum* Moreno-Ruiz		o	o	o	o
T. nitzschioides var. 1 *sensu* Zielinski et Gersonde	3.45	o	o	*	0.16
Thalassiosira antarctica Comber		*	o	*	0.09
T. decipiens (Grunow ex Van Heurck) Jørgensen		o	o	o	0.17
T. eccentrica (Ehrenberg) Cleve		o	0.2	o	o
T. ferelineata Hasle et Fryxell		o	o	o	o
T. gracilis var. *expecta* (Van Landingham) Frxyell et Hasle		5.20	0.4	7.09	o
T. gracilis var. *gracilis* (Karsten) Hustedt		1.40	3.6		o
T. gracilis group		o	4.1	o	1.67
T. gravida Cleve	6.97	0.43	*	0.14	0.12
T. lentiginosa (Janisch) Fryxell	2.79	1.26	5	0.81	0.27
T. leptopus (Grunow ex Van Heurck) Hasle et Fryxell		o	*	o	o
T. lineata Jousé		o	o	o	o
T. maculata Fryxell et Johans		o	*	o	o
T. oestrupii (Ostenfeld) Hasle var. *oestrupii* Fryxell et Hasle		*	*	0.13	0.02
T. oestrupii (Ostenfeld) Hasle var. *venrickae* Fryxell et Hasle			o		o
T. oliveriana (O'Meara) Makarova et Nikolaev		*	0.7	o	0.07
T. symmetrica Fryxell et Hasle		o	o	o	o
T. trifulta Fryxell		0.11	o	o	o
T. tumida (Janisch) Hasle		*	0.1	o	o
Thalassiosira sp. 1		o	*	o	o
Thalassiosira sp. 2		o	o	o	o
Thalassiosira sp. 3		o	o	o	o
Thalassiosira eccentric group		o	o	o	o
Thalassiosira. linear group		o	0.1	o	o
T. trifulta group		o	o	o	o
Thalassiosira spp. < 20 µm		o	0.4	*	o
Thalassiosira spp. > 20 µm		o	*		o
Thalassiothrix antarctica Schimper ex Karsten		o	0.2	0.20	0.23
Thalassiothrix longissima + antarctica		0.46	o	o	o
Trachyneis aspera (Ehrenberg) Cleve		o	o	o	o
Trichotoxon reinboldii (Van Heurck) Reid et Round		*	o	*	0.10
Tropidoneis group		o	*	o	o
Other centrics		*	*	o	o
Other pennates		*	0.1	o	o

	Total Chl-*a* concentration	Sea ice cover	Total diatom flux	*F. kerguelensis* flux	Small *Fragilariopsis* group flux	Biogenic Silica flux	POC flux	POC flux normalized at 2000m
Total Chl-*a* concentration	1.000 p= ---							
Sea ice cover	-0.029 p=.964	1.000 p= ---						
Total diatom flux	0.891 p=.043	-0.433 p=.467	1.000 p= ---					
F. kerguelensis flux	0.218 p=.724	-0.960 p=.010	0.588 p=.297	1.000 p= ---				
Small *Fragilariopsis* group flux	0.944 p=.016	-0.235 p=.703	0.977 p=.004	0.409 p=.494	1.000 p= ---			
Biogenic Silica flux	-0.056 p=.929	-0.958 p=.010	0.379 p=.529	0.869 p=.056	0.199 p=.749	1.000 p= ---		
POC flux	0.236 p=.702	-0.055 p=.930	0.381 p=.527	-0.008 p=.990	0.433 p=.466	0.297 p=.627	1.000 p= ---	
POC flux normalized at 2000m	0.419 p=.482	-0.637 p=.247	0.730 p=.162	0.787 p=.114	0.650 p=.236	0.588 p=.297	0.244 p=.692	1.000 p= ---

Table 4.

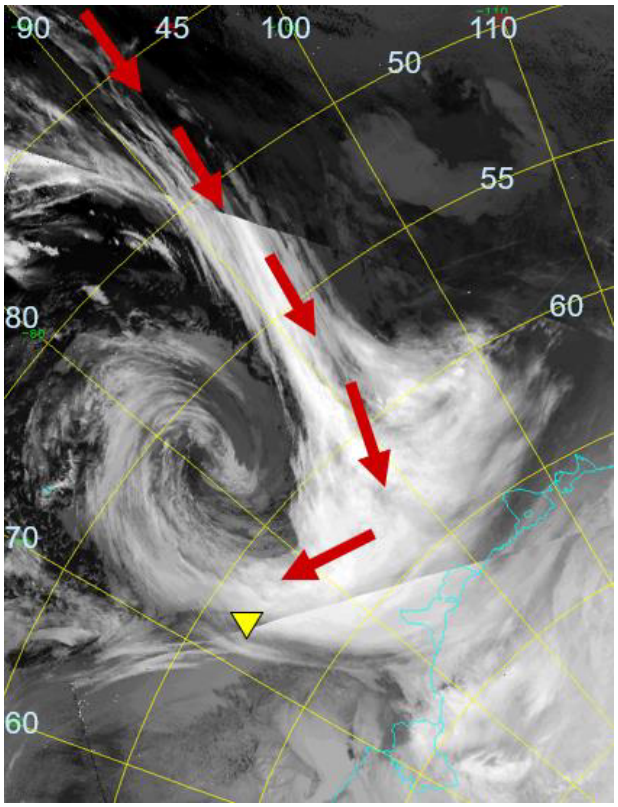

a

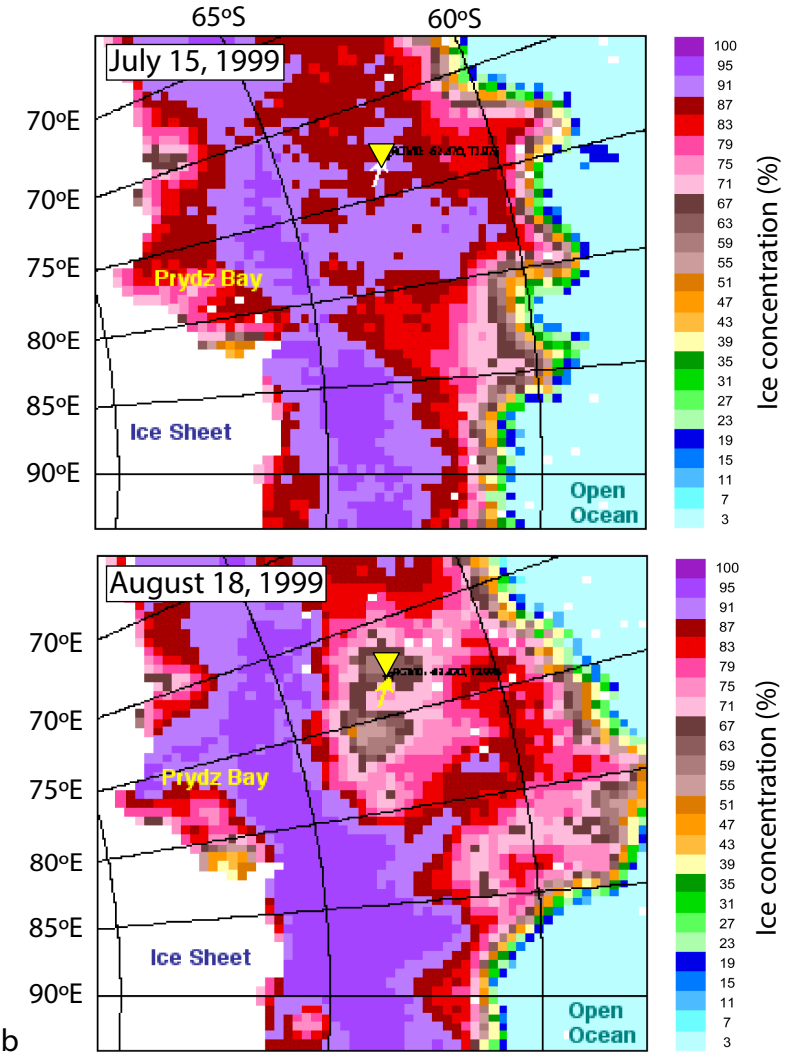

b

Supplementary Figure 1